This is to certify that the

thesis entitled

A SYSTEM'S MODEL FOR A SPARK-IGNITED
INTERNAL COMBUSTION ENGINE

presented by

Yves H.H. Billet

has been accepted towards fulfillment
of the requirements for

Masters degree in Mechanical Engineering

Clark Radcliffe
Major professor

Date 12/15/98

A SYSTEM'S MODEL FOR A SPARK-IGNITED INTERNAL COMBUSTION ENGINE

By

Yves H.H. Billet

A THESIS

Submitted to
Michigan State University
in partial fulfillment of the requirements
for the degree of

MASTER OF SCIENCE

Department of Mechanical Engineering

1998

ABSTRACT

A SYSTEM'S MODEL FOR A SPARK-IGNITED
INTERNAL COMBUSTION ENGINE

By

Yves H.H. Billet

Engine-dynamometer tests provide model data necessary for an engine control system to be established. More specifically, dynamometer tests deliver quantitative relationships between control actions (engine control inputs) and engine performance (engine output). For a spark-ignited, port fuel injected internal combustion engine this document describes a system's framework for the engine subsystems and their signal or power interactions. Steady-state mean value input-output relations for the different subsystems are derived based on dynamometer test data. Engine model control inputs are throttle angle, idle air control, fuel injector pulse width and spark advance. Engine model output performance is formulated in terms of net mechanical power or specific fuel consumption. Experimental procedures are proposed or references provided to obtain all model relations stated.

To my parents

ACKNOWLEDGMENTS

I am very grateful in the first place to my faculty advisor Dr Radcliffe for the full and unconditional support he gave me throughout my education at MSU and during the two thesis projects we ran together. Especially, I would like to thank him for the patience he showed in defining the subject of this thesis and for the backup he gave me in the contacts with other faculty members. Dr Radcliffe, I will always keep in mind the talks we had and the way you responded to the issues I brought up. I have learned more from you than I could ever have hoped to pick up at a university.

I would like to thank Dr Schock for accepting my project at the Hulett Road Engine Research Facility and for supplying the space and equipment necessary to set up a test bed for engine control. I would also like to thank Dr Salam and the NSF group in general for long term support of my research and education.

Special thanks as well to Dr Shaw and Dr Khalil for being understanding towards my position as a teaching assistant, especially during my last semester at MSU. I am convinced that through their amazing efforts, the NSF course is now put on the right track. Dr Khalil and Dr Shaw, I don't recall you having caused any of my after-meeting headaches: thanks for being the quiet guys!

Of course I reserve a special paragraph for my "older brother and battery specialist" Tom Stuecken, who led me through the experimental work and who taught me how to stand the pain of real-life grease monkey trouble-shooting.

Tom, very little at Hulett would be possible without you being around! Thanks for all the time and effort you put into my project!

I am very pleased with the research environment at Hulett Road and its people: Mark, thanks for speeding up the contacts with Ford, your once in a lifetime mass airflow sensor discovery and your never ending burger-mania. Dr Brereton, Hans and Dr Lee, thanks for your interest, daily advice and comments. Rahi, Mischa, Steve it was a lot of fun and everyday irony to have you around!

Thanks as well to Mr. Milz at Cosworth Engineering and Mr. Lorusso at Ford to supply the information necessary to run the engine controller.

Besides, I would like to mention my great companions of the Dynamic Systems Laboratory: Mark, Charles, Byam, Yoga, Joe, Brennan and Gary, you filled my days and nights at the EB with joy and at times very unpredictable madness!

The department secretaries Nancy, Carol, Martha, Aida and Bobby deserve a special note for their everyday enthusiasm and support in administrative matters.

Finally, I would like to express my greatest appreciation towards my international friends at MSU. Lars, Thomas, Ramez, Khash, Laurel, Jim, Bernhard, Kara, Fariba, Taka, Nao, Azu, Takeo, Su, Dae Yong and Natalie: I will never forget the time we spent together! Thank you very very much!!

TABLE OF CONTENTS

LIST OF TABLES

LIST OF FIGURES

KEY TO SYMBOLS OR ABBREVIATIONS

ACT: Air Charge Temperature

AFI : Air Fuel Ratio Influence Function []

$duty_{IAC}$: Idle Air Control Valve Duty cycle [%]

ECT: Engine Coolant Temperature

EDIS: Electronic Distributorless Ignition System

EEC: Electronic Engine Control Module

EGO: Exhaust Gas Oxygen Sensor

EGR: Exhaust Gas Recirculation

FB: Feedback

G : Fuel Injector Flow Conductance [$(m^3/s)/Pa^{1/2}$]

HEGO: Heated Exhaust Gas Oxygen Sensor

IAC: Idle Air Control

L.E.D.: Light Emitting Diode

$\dot{m}$: MAF Sensor Airflow [kg/hr]

$\dot{m}_a$: Mass Airflow [kg/hr]

m_{ac} : Cylinder Air Charge [kg]

$\dot{m}_{ai}$: Mass Airflow into the Intake Manifold [kg/s]

$\dot{m}_{ao}$: Mass Airflow out of the Intake Manifold [kg/s]

$\dot{m}_f$: Fuel Flow Rate [kg/hr]

m_{fc} : Cylinder Fuel Mass [kg]

$(m_{fc})_{stoich}$: Cylinder Fuel Mass at Stoichiometry [kg]

$\dot{m}_{fi}$: Fuel Injector Mass Flow Rate [kg/hr]

n: number of cylinders

n_i: number of the spark plug in the firing sequence

MAF: Mass Airflow

MBT : Minimum Spark Advance for Best Timing [deg crank BTDC compression]

offset: Fuel Injector Offset [ms]

p : Pressure [Pa]

P_b : Engine-Dynamometer Power Transfer [Nm/s]

P
P
P
P
P
P
P
P
P
Q
Q
Q
Q
r.
R
R_E
R
R
R
S
S
SF
sf
T
T_A
T_b
T_b
T_b
T_E
T_i
T_m
T_o
TP

P/E: Position/Excitation

p_f: Pressure Upstream of the Fuel Injector [Pa]

P_f: Mechanical Loss Power [Nm/s]

P_i: Gross Indicated Power [Nm/s]

p_m: Manifold Pressure [Pa]

P_{net}: Net Available Mechanical Power [Nm/s]

p_0: Environmental Pressure [Pa]

PW: injector pulse width [ms]

Q: Volumetric Flow [m^3/s]

Q_f: Volumetric Fuel Flow into the Intake Runner [m^3/s]

Q_{hv}: Lower Heating Value of the Fuel = 44.0 MJ/kg

Q_{io}: Fuel Injector Volumetric Flow [m^3/s]

r: Ideal Gas Constant of Air = 287 J/(kg K)

R_{ACT}: ACT Sensor Resistance [kΩ]

R_{ECT}: ECT Sensor Resistance [kΩ]

R_{HEGO}: HEGO Heating Resistance [Ω]

RPM: Engine speed [rot/min]

R_{TPS}: Throttle Position Sensor Resistance [kΩ]

SA: Spark Advance [DBTDC compression]

SAI: Spark Advance Influence Function []

SP: Set Point

sfc: Specific Fuel Consumption [mg/Nm or (g/s)/kW]

T: Torque [Nm]

T_{ACT}: Air Charge Temperature [°C]

T_b: Brake Torque [Nm]

T_{bdes}: Desired Dynamometer Load Torque [Nm]

T_{block}: engine block temperature [K]

T_{ECT}: Engine Coolant Temperature [°C]

T_i: Gross Indicated Torque [Nm]

T_m: manifold temperature [K]

T_0: Environmental Temperature [K]

TPS: Throttle Position Sensor

V_c: Displaced Cylinder Volume [m^3]

V_{ref}: Mass Airflow Sensor Supply Voltage [volt]

W_{actual} : Actual Work available Mechanically over a Combustion Event [Nm]

W_{ideal}: Ideal Work available Thermally over a Combustion Event [Nm]

WOT: Wide Open Throttle

XFB: External Feedback

η_f: Indicated Fuel Conversion Efficiency []

$\eta_{f|stoich}$: Stoichiometric Fuel Efficiency []

η_m : Mechanical Efficiency []

θ : Throttle Angle [deg]

θ ': Dimensionless Throttle []

θ_{WOT}: Throttle Angle at Wide Open Throttle [deg], 88.9 º

λ : Relative Air to Fuel Ratio = $(A/F)/(A/F)_{stoich}$

ρ_f : Fuel Density [kg/m^3]

ω : Angular Velocity [rad/s]

ω_{des} : Desired Dynamometer Angular Speed [rad/s]

ω_e: Crankshaft Angular Velocity [rad/s]

ω_e': Dimensionless Engine Speed

ω_{nom}: Nominal Engine Speed [rad/s], 4500 RPM

INTRODUCTION

Government mileage and emission regulations for spark-ignited combustion engines have left automotive engineers with a complicated optimization task [Ribbens, 1998]. Most automobile engine inventions date from the first half of the 20th century. Long-term experience has led to continuous and extensive design optimization of mechanical and electrical subsystems [Hempson, 1976, Heywood, 1988]. Research and testing efforts associated with incremental changes in engine performance through design adjustments have however grown tremendously.

Systems and controls engineers take an alternative, active, route in the optimization process. The idea is to allow for engine design limitations but to compensate for these by steering the engine into optimal performance by means of feedback controlled engine operation. Control actions are taken based on engine modeling information and on-line measurements. Control models typically covers the physical behavior and interaction of the engine subsystems. Powell (1987), Powell and Cook (1983), Huang and Velinsky (1993) give an extensive overview of the field of spark-ignited engine modeling for application in electronic engine control.

Model information is commonly extracted from engine-dynamometer test data [Tennant, Giacomazzi, 1979]. This document describes a system's framework to establish the functional relationships between control inputs and engine output performance. Engine control inputs are: idle air control (IAC), throttle, fuel

injection timing and ignition timing. Performance is formulated in terms of mechanical power or specific fuel consumption and related to measurable quantities in an engine-dynamometer test.

An engine-dynamometer test bed was constructed to provide model data. Tests were run on the 1995 1.9 liter Ford Escort driven by its own electronic engine control module. Tests requiring changes in spark or fuel injection timing were conducted using the Cosworth Intelligent Controls IC5460 Engine Control System ®.

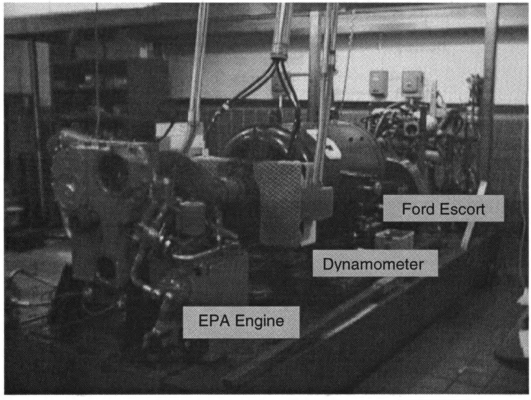

Fig.1: Overview of the Facility (Construction Stage)

The facility (Fig.1) consisted of a bi-directional DC dynamometer and dynamometer control system, which could quickly switch operation between the

Ford Escort engine and a research engine for the Environmental Protection Agency. The Cosworth IC5460 Engine Control System ® was shared between the two engines (Fig.2). Test results are discussed in the main document. The appendices contain details on operation of the facility and listing of test data.

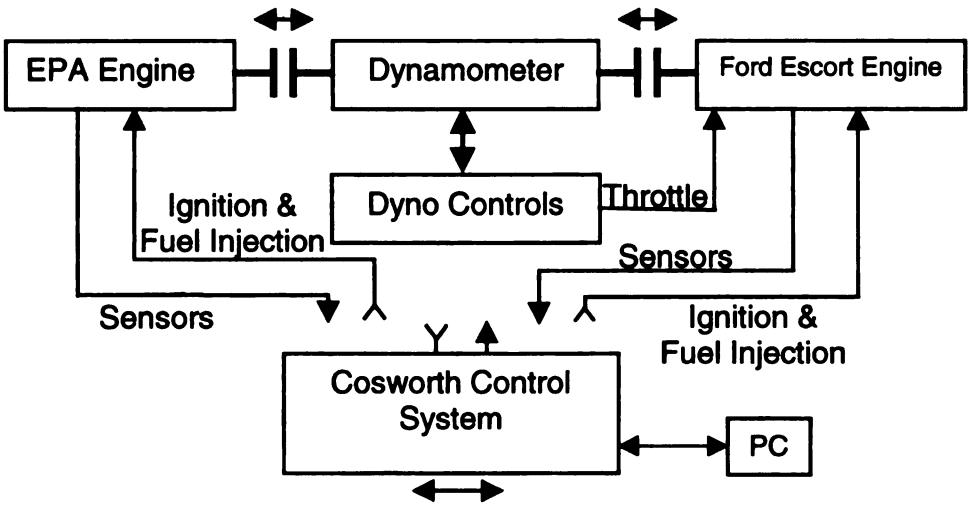

Fig.2: Schematic of the Facility

Chapter 1

MECHANICAL SYSTEMS INTERACTION

The control model relationships between engine output performance and engine control inputs are derived in several steps. The engine is subdivided into a set of interacting subsystems of lesser size and model complexity. The subsystems are subsequently characterized through dynamometer measurements. This is done in an ordered manner, starting with the output side of the engine (engine performance) and working back to the input side (control inputs). Steady engine operation is considered only: the engine is not accelerating. All model relations are formulated in terms of mean quantities over time.

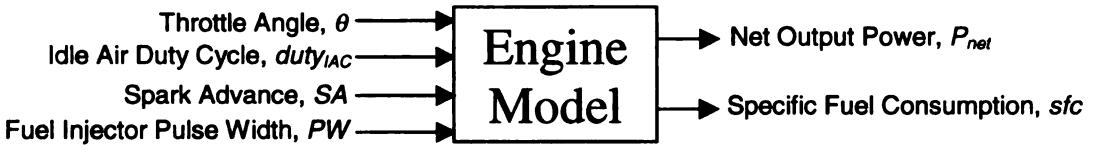

Fig.3: Overall Model Structure

The overall model structure (Fig.3) has the following inputs: throttle angle (θ), idle air control valve duty cycle ($duty_{IAC}$), spark advance (SA) and fuel injector pulse width (PW). The model outputs are the net mechanical engine power P_{net} and the specific fuel consumption *sfc*.

The engine-dynamometer mechanical power flow (Fig.4) is driven by the gross indicated power (P_i). The gross indicated power is distributed over three subsystems: the mechanical dynamics, the mechanical losses (P_f) and the dynamometer (P_b).

The dynamometer brake power P_b represents the power transfer to the dynamometer through the engine-dynamometer shaft coupling. An electrical dynamometer can both absorb power (generator mode) and supply power (motor mode). We will assume P_b is positive when flowing into the dynamometer. If the engine overcomes its mechanical losses when firing, the direction of the power transfer P_b depends on whether engine ignition is activated or not.

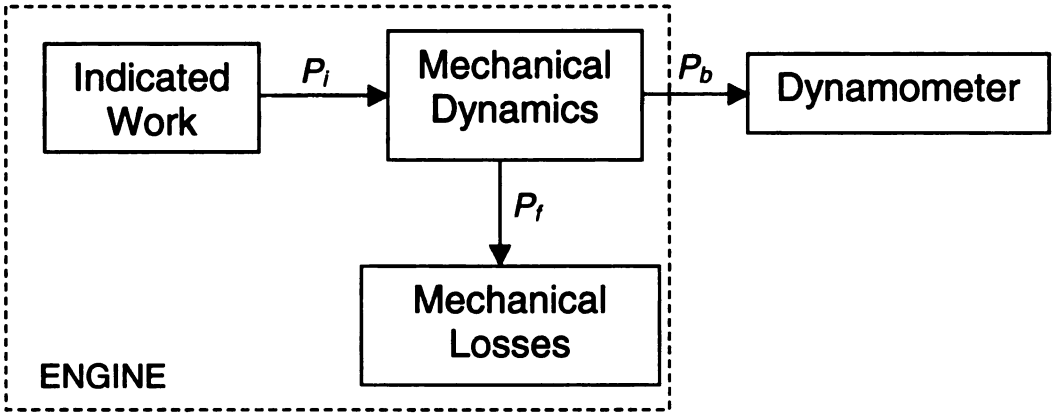

Fig.4: Engine-Dynamometer Mechanical Power Flow

The mechanical loss power P_f accounts for friction losses and also includes the pumping work of the engine during intake and exhaust strokes.

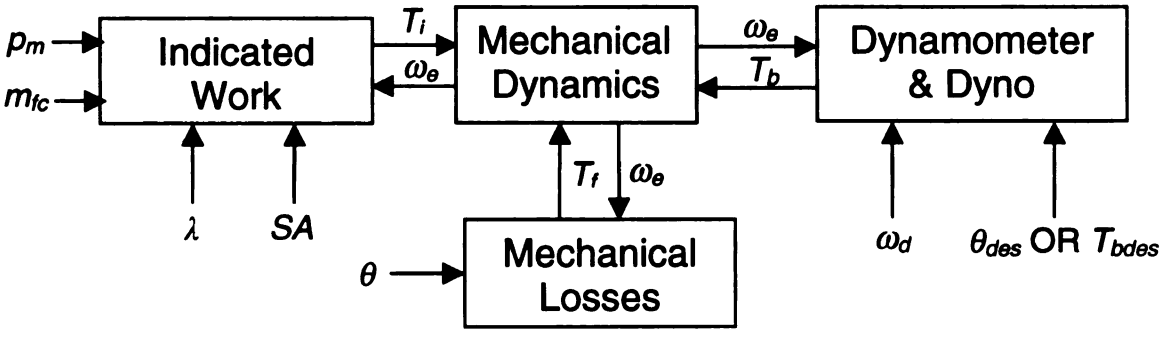

Fig.5: Mechanical Systems Power and Signal Interaction

Mechanical power interactions are expanded into pairs of power variables (torque T and angular speed ω) in Fig.5. The causal relationships indicated by the arrow pairs define which of the power variables are input variables and which are output variables to the separate subsystems. The *Mechanical Dynamics* have the angular speed ω_e as a kinetic energy storage variable: speed is the natural output variable of the *Mechanical Dynamics* subsystem. Causality requires all torque interactions to be input variables to the *Mechanical Dynamics* subsystem.

Signal level interaction between subsystems (Fig.5) does not have significant power flow associated with it. Unlike power interactions, signal interactions are represented by single arrows. Karnopp and Margolis (1990) give a discussion of system modeling based on causality, power and signal interactions. We will now develop the relation between input and output variables for the different subsystems.

The *Dynamometer* is a controlled device. The dynamometer control system sets the brake torque T_b as a function of the input variables to the dynamometer control system. The user specifies the desired engine speed ω_{des}. In addition, the user is given control over the power interaction between engine and dynamometer by setting the power produced by the engine or by setting the power absorbed by the dynamometer. Control over the power produced by the engine is given by means of the throttle angle θ. Control over the power absorbed by the dynamometer is given by means of the brake torque T_b. The

user then specifies either a desired throttle angle θ_{des} or a desired brake torque T_{bdes}.

The dynamometer control system measures the shaft rotational speed ω_e and compares this speed to the desired value ω_{des}. In the control mode of specified throttle angle (θ_{des}), the dynamometer control system sets the throttle angle at the user-specified value θ_{des} and adjusts the brake torque T_b until the speed error becomes zero. In the control mode of specified load torque (T_{bdes}), the dynamometer control system sets the brake torque T_b at the user-specified value T_{bdes} and adjusts the throttle angle θ until the speed error becomes zero. If even at wide-open throttle (WOT) the engine cannot generate the specified brake torque T_{bdes}, the dynamometer will fully open the throttle and reduce the brake torque to a value lower than the specified value T_{bdes}.

The *Mechanical Losses* block has the friction torque T_f as an output variable and crankshaft angular velocity ω_e and throttle angle θ as input variables. A functional relationship of the form

$$T_f = f_1(\theta, \omega_e) \tag{1}$$

is proposed. Dependency on engine speed accounts for viscous friction as well as for the variation of the pumping losses with engine speed. Dependency on throttle angle accounts for the variation of the pumping losses in the intake system with the throttle position. Effects not included in the model are other quantities influencing friction, such as pressure inside the cylinder and valvetrain

loading. The model assumes that piston ring friction and valvetrain loading are not significantly different under variations in cylinder pressure.

The *Indicated Work* block represents the mechanical power production from the combustion process. It has the gross indicated torque (T_i) as an output variable and crankshaft angular velocity (ω_e), mean manifold pressure (p_m), cylinder fuel mass (m_{fc}), relative air to fuel ratio (λ) and spark advance (SA) as input variables. At steady operation we propose a functional relationship of the form

$$T_i = f_2(m_{fc}, p_m, \omega_e, \lambda, SA) \tag{2}$$

The gross indicated torque also depends on other quantities such as heat transfer and exhaust gas recirculation. We will however only study the influence of the quantities given in (2).

At steady operation, the engine is not accelerating and the kinetic energy of the mechanical dynamics is constant: the gross indicated power equals the sum of the loss power and the brake power:

$$P_i = P_f + P_b \tag{3}$$

Input-output power flows of the *Mechanical Dynamics* block (Fig.5) all have the same associated speed ω_e. The power conservation (3) can therefor also be expressed in terms of torque:

$$T_i = T_f + T_b \tag{4}$$

A friction torque estimate (Fig.6) was obtained by turning off the ignition ($T_i = 0$) and running dynamometer tests for several throttle conditions θ_{des} at different speed set points ω_{des}. The model estimate assumes that piston ring friction and

valvetrain loading are not significantly different in the motored configuration than in the firing configuration. Temperature effects on oil and coolant viscosity were reduced by bringing the engine back to its operating temperature in between a series of measurements. Block temperature was still found to vary between 175°F and 195°F during motoring. Measured friction torque data (Fig.6) are shown as a function of dimensionless throttle ($\theta'=\theta/\theta_{WOT}$, θ_{WOT} = 88.9°) and dimensionless speed ($\omega'=\omega/\omega_{nom}$, ω_{nom} = 4500 RPM).

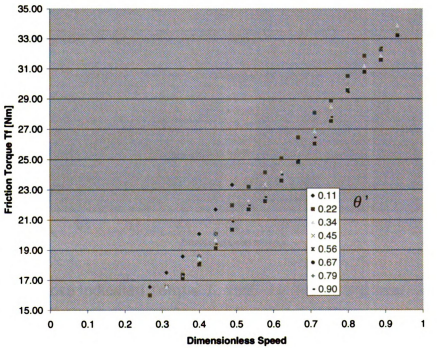

Fig.6: Measured Friction Torque T_f, 1995 1.9 liter Ford Escort

The friction torque (Fig.6) predominantly varies linearly with engine speed, indicating viscous effects. For lower throttle angles, the friction increases due to the increased pumping losses in the intake. Quadratic pumping loss dependency on engine speed starts to show at lower throttle angles.

The gross indicated torque (T_i) for a firing engine (Fig.7) is obtained by adding the friction torque estimate T_f (Fig.6) to the dynamometer brake torque reading (T_b). Fig.7 shows calculated gross indicated torque as a function of dimensionless speed (ω_e') and dimensionless throttle (θ').

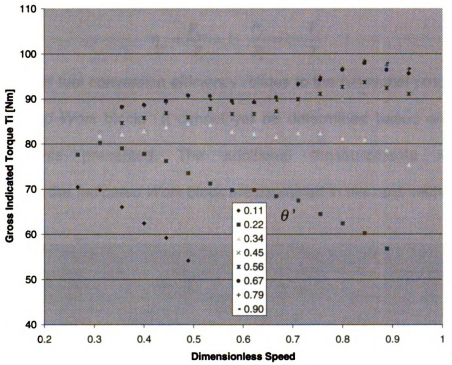

Fig.7: Gross Indicated Torque T_i, 1995 1.9 liter Ford Escort, using (4)

Engine output performance in terms of net available mechanical output power (P_{net}) or specific fuel consumption (*sfc*) is directly related to the measured quantities T_b and T_f. The engine net output power equals the brake power:

$$P_{net} = P_b = T_b \cdot \omega_e \tag{6}$$

The specific fuel consumption (*sfc*) as a measure of mileage is inversely proportional to the product of the mechanical efficiency (η_m) and the indicated fuel conversion efficiency (η_i):

$$sfc = \frac{1}{\eta_m \cdot \eta_f \cdot Q_{hv}} \tag{7}$$

with Q_{hv} the lower heating value of the fuel.

Mechanical efficiency (Fig.8) follows from the dynamometer measurements T_i and T_f:

$$\eta_m = \frac{P_{net}}{P_i} = 1 - \frac{P_f}{P_i} = 1 - \frac{T_f}{T_i} \tag{8}$$

The indicated fuel conversion efficiency relates to the functional properties (2) of the *Indicated Work* block. It cannot yet be determined based on the torque measurements presented. The additional measurements required to characterize the *Indicated Work* block are explained in the next section.

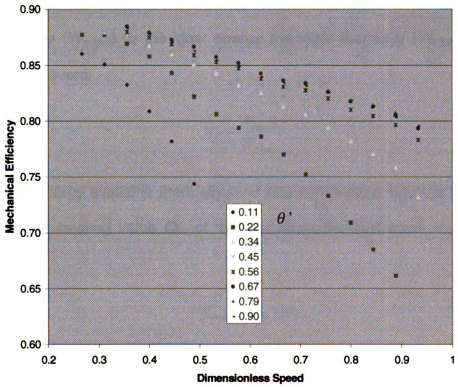

Fig. 8: Mechanical Efficiency, 1995 1.9 liter Ford Escort, using (8)

Chapter 2

INDICATED WORK AND INDICATED FUEL CONVERSION EFFICIENCY

The *Indicated Work* block and the indicated fuel conversion efficiency η_f will now be studied in detail to generate an expansion for the gross indicated torque function (2). We will adapt the structure proposed by Dobner (1980) and further expanded by Chang (1988) and Moskwa (1987). Their model for the gross indicated torque function (2) separates the influence of the inputs to the *Indicated Work* block on torque production based on quasi-physical considerations.

The indicated fuel conversion efficiency η_f is the ratio of the energy produced mechanically (W_{actual}) to the ideal energy available thermally (W_{ideal}) over one combustion event:

$$\eta_f = \frac{W_{actual}}{W_{ideal}} \tag{9}$$

The ideal energy available thermally over one combustion event is taken equal to the lower heating value Q_{hv} of the fuel times the fuel mass m_{fc} inside the cylinder:

$$W_{ideal} = Q_{hv} \cdot m_{fc} \tag{10}$$

The actual work produced mechanically over one combustion event equals the gross indicated power P_i divided by the number of combustion events per

second. For a four-stroke engine with n cylinders the actual work produced becomes:

$$W_{actual} = 4\pi \cdot \frac{P_i}{n \cdot \omega_e} \tag{11}$$

The gross indicated power P_i equals the gross indicated torque T_i times the angular speed ω_e, with (11):

$$W_{actual} = 4\pi \cdot \frac{T_i}{n} \tag{12}$$

The indicated fuel conversion can be evaluated with (9), (10), (12):

$$\eta_f = \frac{4\pi \cdot T_i}{n \cdot \omega_e \cdot Q_{hv} \cdot m_{fc}} \tag{13}$$

A model for the indicated fuel conversion efficiency as a function of the *Indicated Work* block inputs is presented. As shown by Chang (1988) through combustion simulations, the indicated fuel conversion efficiency can be expanded as the product of a spark advance influence factor *SAI*, a relative air to fuel ratio influence factor *AFI* and the stoichiometric fuel conversion efficiency $\eta_{f|stoich}$:

$$\eta_f = \eta_{f|stoich} \cdot AFI \cdot SAI \tag{14}$$

The stoichiometric fuel conversion efficiency equals the indicated fuel conversion efficiency with the relative air to fuel ratio λ at stoichiometry (λ=1) and the spark advance *SA* at its Minimum advance for Best Timing (*MBT*). The stoichiometric fuel conversion efficiency depends on intake conditions (mean manifold pressure p_m) and engine speed (ω_e):

$$\eta_{f|stoich} = \eta_{f|stoich}(p_m, \omega_e) \tag{15}$$

The *SAI* and *AFI* multipliers model efficiency deviations from the reference conditions (*SA* = *MBT*, $\lambda = 1$):

$$AFI = AFI(\lambda) \tag{16}$$

$$SAI = SAI(SA - MBT) \tag{17}$$

Through the definitions of *AFI* and *SAI*

$$AFI(1) = 1, SAI(0) = 1 \tag{18}$$

Calculation of the functions (15), (16) and (17) is done using (13) combined with (14):

$$\eta_f\big|_{stoich}(p_m, \omega_e) \cdot AFI(\lambda) \cdot SAI(SA - MBT) = \frac{4\pi \cdot T_i}{n \cdot \omega_e \cdot Q_{hv} \cdot m_{fc}} \tag{19}$$

To characterize the *SAI* multiplier, it suffices to hold the relative air to fuel ratio (λ), the mean manifold pressure (p_m), and the engine speed (ω_e) at arbitrary but fixed values and to measure the variation in gross indicated torque (T_i) due to changes in the spark advance (*SA*) with respect to *MBT*. The *SAI* multiplier for the measurements in the above procedure is obtained by dividing (19) through its value at *MBT*, with (18):

$$SAI(SA - MBT) = \frac{T_i}{T_i\big|_{SA=MBT}} \tag{20}$$

Fig.9: SAI Multiplier, 1995 1.9 liter Ford Escort, using (20)

Experimental values and a quadratic least square curve fit for the *SAI* multiplier are given in Fig.9. The highest value for the efficiency occurs at *MBT* (*SA-MBT*= 0).

To measure the *AFI* multiplier, it suffices to hold the spark advance (*SA*), the mean manifold pressure (p_m), and the engine speed (ω_e) at arbitrary but fixed values and to measure the variation in gross indicated torque (T_i) due to changes in the relative air to fuel ratio (λ) with respect to stoichiometry. For fixed intake conditions (fixed manifold pressure and air charge), a change in λ implies a change in cylinder fuel mass (m_{fc}). The *AFI* multiplier for the measurements in the above procedure is obtained by dividing (19) through its value at stoichiometry, with (18):

(21)

Experimental values and a least square polynomial curve fit for the *AFI* multiplier are given in Fig.10. A sixth order polynomial was required to accurately capture the maximum of the curve and the *AFI* value of 1 at stoichiometry. The highest efficiency occurs for a slightly lean mixture ($\lambda > 1$).

Calculation of the stoichiometric fuel conversion efficiency is done using (19). The stoichiometric fuel conversion efficiency is mapped for a set of intake (p_m) and engine speed (ω_e) conditions at arbitrary *A/F* ratio and arbitrary *SA*. At all mapping conditions, *A/F* ratio and *SA* are calculated and the *SAI* and *AFI* multipliers evaluated using the curve fits of Fig.9 and Fig.10.

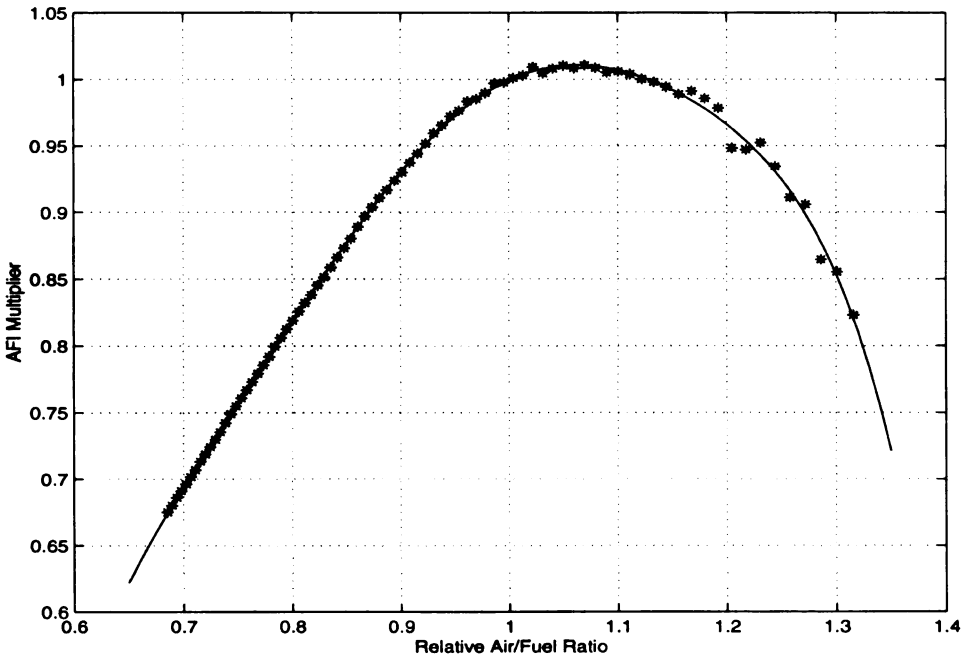

Fig.10: AFI Multiplier, 1995 1.9 liter Ford Escort, using (21)

There are three fundamental problems with this approach to calculation of the stoichiometric fuel conversion efficiency. First, *SAI* multiplier evaluation is not

straightforward because *MBT* is dependent on both cylinder air charge (m_{ac}) and engine speed (ω_e):

$$MBT = MBT(m_{ac}, \omega_e) \tag{22}$$

Second, *AFI* multiplier evaluation is not straightforward because the relative air to fuel ratio λ is:

$$\lambda = \frac{(m_{fc})_{stoich}}{m_{fc}} \tag{23}$$

with m_{fc} and $(m_{fc})_{stoich}$ the actual fuel mass in the cylinder and the fuel mass in the cylinder at stoichiometry. Evaluation of (23) requires measurement of the in-cylinder fuel mass. Finally, mapping of the stoichiometric fuel conversion efficiency using (19), even for known *AFI* and *SAI* also requires measurement of the in-cylinder fuel mass m_{fc}.

Determination of the in-cylinder air charge (m_{ac}) and the in cylinder fuel mass (m_{fc}) as required for the evaluation of *AFI*, the evaluation of *SAI* and the mapping of $\eta_{f|stoich}$ cannot be done through direct measurement. The next section gives a procedure to measure the cylinder fuel mass and a way to estimate the cylinder air charge, as related to the pulse width (*PW*) command of the fuel injection system.

Chapter 3

FUEL INJECTION SYSTEM

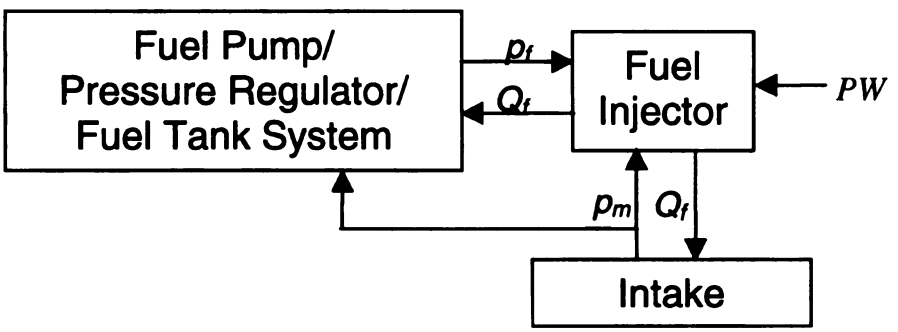

Fig.11: Port Fuel Injection System

The cylinder fuel mass (m_{fc}) is required for mapping of the stoichiometric fuel conversion efficiency (19) and for evaluation of the *AFI* multiplier (21). It cannot be measured directly, but it depends on the injector pulse width control (*PW*) of the fuel injection system (Fig.11). The causal relations between the different fuel injection subsystems are presented in Fig.11. Power flow interactions are formulated through pairs of power variables (pressure p and volumetric flow Q).

The *pressure regulator* controls the pressure p_f upstream of the injector based on a pressure signal p_m from the intake manifold. The pressure p_f is regulated such that the pressure drop $\Delta p_{des} = p_f - p_m$ across the fuel injector stays constant. The flow through the fuel injector depends on the pressure drop $\Delta p = p_f - p_m$ across the injector. Due to the action of the pressure regulator $\Delta p = \Delta p_{des}$, such that the injector volumetric flow rate becomes:

$$Q_{io} = G \cdot \sqrt{\Delta p_{des}} \tag{24}$$

The electronic control unit applies a voltage pulse to the fuel injector with pulse width *PW*. The mass of fuel injected during an injection event is equal to:

$$m_{fc} = (PW - offset) \cdot \rho_f \cdot Q_{io} = (PW - offset) \cdot \dot{m}_{fi} \tag{25}$$

ρ_f is the fuel density and ($\dot{m}_{fi}$) the injector mass flow rate. The value *offset* refers to the opening time of the injector.

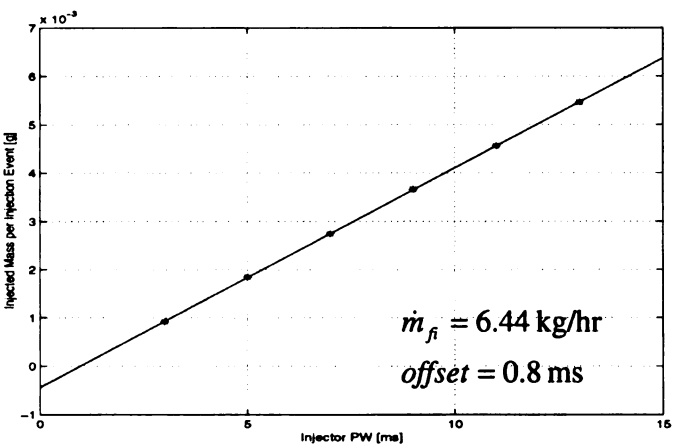

Fig. 12: Fuel Injector Calibration, 1995 1.9 liter Ford Escort, using (25)

Measurement of the injector flow rate $\dot{m}_{fi}$ and the injector offset was done in a flow bench test. During the test, an injector is fired a preset number of times with a known pulse width *PW*. The fuel mass per injection event is recorded by weighting. The mass per injection is plotted versus pulse width (Fig.12) and a linear least square fit is obtained. The injector flow rate depends on the pressure drop (24): during the calibration test, the pressure drop must equal the value Δp_{des} imposed by the pressure regulator in a firing engine. The injector flow rate $\dot{m}_{fi}$ is found as the slope of the linear curve. The injector *offset* is found as the intersection of the linear curve with the *PW* axis.

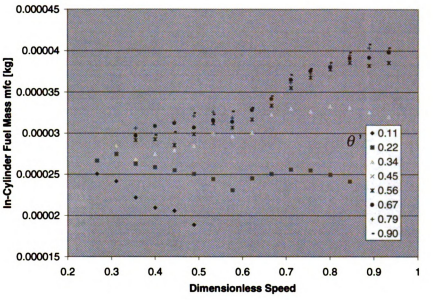

Fig.13: Measurement of the In-cylinder Fuel Mass m_{fc}, 1995 1.9 liter Ford Escort

The in-cylinder fuel mass (Fig.13) for the operating conditions of Fig.7 is determined in a dynamometer test by measurement of the injector *PW* during steady operation and application of (25). Fig.13 reflects the base fuel settings of the engine control system as a function of dimensionless throttle and dimensionless speed (ω_e'). An average value for the *PW* was recorded to average out the effect of the exhaust gas oxygen feedback control on the injector pulse width.

The indicated fuel conversion efficiency η_f (Fig.14) can now be determined as a function of dimensionless speed (ω_e') and dimensionless throttle (θ ') by combining the in-cylinder fuel mass (Fig.13) with the gross indicated torque (Fig.7) through application of (13).

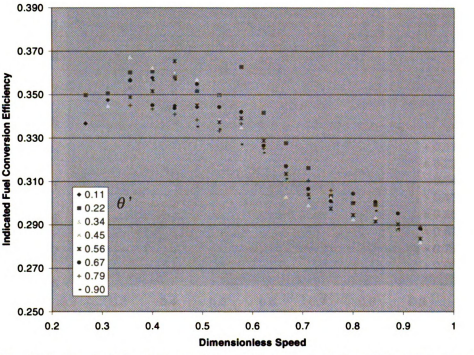

Fig.14: Indicated Fuel Conversion Efficiency,1995 1.9 liter Ford Escort, using (13)

The in-cylinder fuel mass at stoichiometry $(m_{fc})_{stoich}$ (Fig.15) is determined by measurement of the injector *PW* at stoichiometry and application of (21). Stoichiometric conditions were estimated using the signal from the Heated Exhaust Gas Oxygen (HEGO) sensor. The injector *PW* was varied until the HEGO sensor started to switch between rich and lean voltage levels. The *PW* at stoichiometry was taken as the *PW* for which the HEGO sensor signal on average stays rich and lean for an equal amount of time.

The relative air to fuel ratio λ (Fig.16) is found out of the measurements of the cylinder fuel mass (Fig.13) and the cylinder fuel mass at stoechiometry (Fig.15) with application of (18). The *AFI* multiplier at the measurement points of Fig.7 can now be evaluated using the SAI curve fit of Fig.10.

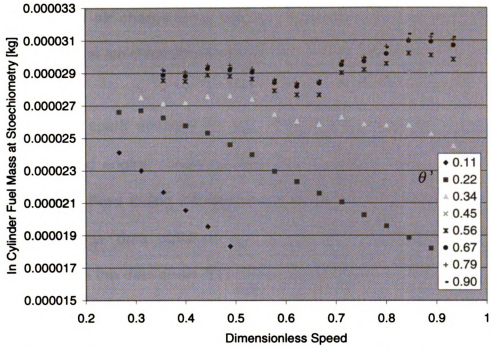

Fig. 15: Measurement of the In-Cylinder Fuel Mass at Stoichiometry, 1995 1.9 liter Ford Escort (stoichiometry was estimated using the signal from the HEGO)

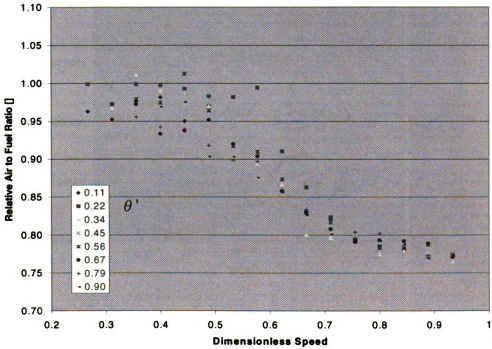

Fig.16: Relative Air to Fuel Ratio λ, 1995 1.9 liter Ford Escort, using (23)

The in-cylinder air charge (m_{ac}) (Fig.17) is proportional to the in-cylinder fuel mass $(m_{fc})_{stoich}$ at stoichiometry (Fig.15):

$$m_{ac} = 14.6 \cdot (m_{fc})_{stoich} \tag{26}$$

The minimum spark advance for best timing (*MBT*) depends on cylinder air charge m_{ac} and engine speed ω_e (22). The map (22) was not generated but obtained from Ford timing information on the 1990 1.9 liter Ford Escort. For every air charge data point of Fig.17, *MBT* was evaluated through linear interpolation on the data sheet from Ford for zero EGR. Fig.18 gives the results as a function of dimensionless speed (ω_e') and dimensionless throttle (θ ').

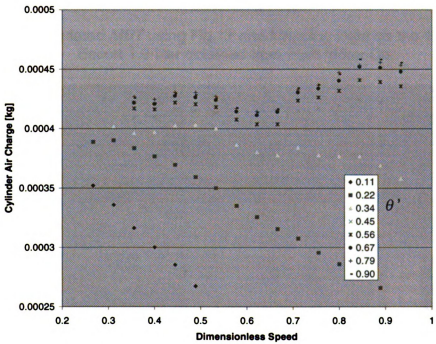

Fig.17: Cylinder Air Charge m_{ac}, 1995 Ford Escort 1.9 liter, using (26)

The *SAI* multiplier at the measurement point of Fig.7 can now be evaluated using the SAI curve fit of Fig.9 and the *MBT* values of Fig.18.

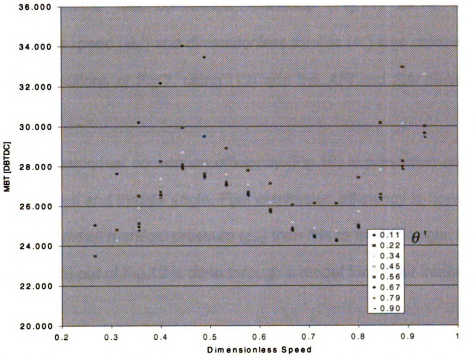

Fig.18: Calculated *MBT* using Fig.17 and Mapping Data on the 1990 Ford Escort 1.9 liter obtained from Ford Motor Co.

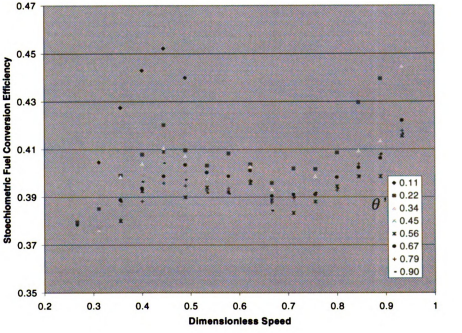

Fig.19: Stoichiometric Fuel Conversion Efficiency, 1995 1.9 liter Ford Escort, using (19) and Curve Fits of Fig.9 and Fig.10

The stoichiometric fuel conversion efficiency (Fig.19) as a function of dimensionless speed (ω_e') and dimensionless throttle (θ ') was calculated for the operating conditions of Fig.7, using (19) and the *AFI* and *SAI* curves of Fig.9 and Fig.10.

The stoichiometric fuel conversion efficiency (Fig.19) is presented as a function of engine speed and throttle angle. Fuel conversion efficiency is however rather related to the mean manifold pressure (p_m) than it is to throttle angle. Generation of the map (15) out of Fig.19 is done through a model for the air intake system.

Chapter 4

AIR INTAKE SYSTEM

The results for the stoichiometric fuel conversion efficiency (Fig.19) were given as a function of throttle angle and engine speed. The data in Fig.19 give fuel conversion efficiency for an engine with idle air control active. Each data point in Fig.19 corresponds to a certain combination of throttle and idle air control. Representation of efficiency as a function of throttle angle only is less general. To avoid a multi-dimensional map of efficiency as a function of throttle angle, engine speed and idle air control, manifold pressure and engine speed are used instead as the independent variables to characterize the stoichiometric fuel conversion efficiency.

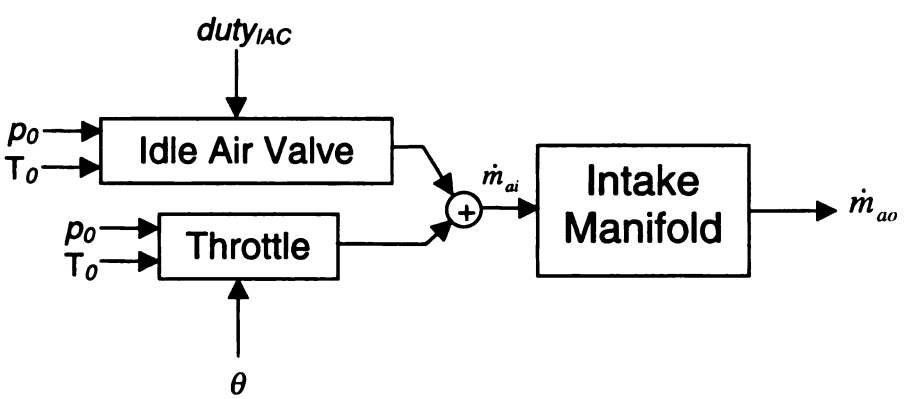

Fig.20: Air Intake System Signal Flow

The air intake system will be studied to relate the mean manifold pressure p_m to the control inputs of the induction system: the throttle angle (θ) and the idle air control valve duty cycle ($duty_{IAC}$). This will allow conversion of the

stoichiometric fuel efficiency results of Fig.19 into a map with manifold pressure and engine speed as independent variables.

A signal flow scheme for the air intake system (Fig.20) consists of the idle air valve, the throttle and the intake manifold. Moskwa and Hedrick (1989) give detailed model relations for the airflow into the manifold as a function of idle air valve duty cycle, throttle angle, environmental pressure (p_0) and environmental temperature (T_0). In general, one could write:

$$\dot{m}_{ai} = \dot{m}_{ai}\,(duty_{IAC},\ \theta,\ p_m,\ p_0,\ T_0) \tag{27}$$

The mean mass airflow ($\dot{m}_{ao}$) out of the intake manifold equals the cylinder air charge (m_{ac}) times the number of cylinder fillings per second. For a four-stroke engine with n cylinders:

$$\dot{m}_{ao} = m_{ac} \cdot \frac{n \cdot \omega_e}{4\pi} \tag{28}$$

The cylinder air charge (m_{ac}) depends on different factors, such as manifold pressure and temperature, exhaust gas pressure, engine speed, etc. [Heywood, 1986, Servati, 1986]. For purpose of our analysis, we will assume dependency of the air charge on manifold pressure and engine speed only.

$$m_{ac} = m_{ac}(p_m, \omega_e) \tag{29}$$

At steady operation, the mass airflow $\dot{m}_{ai}$ into the intake manifold must equal the airflow $\dot{m}_{ao}$ out of the intake manifold. With (27), (28) and (29):

$$\dot{m}_{ai}(duty_{IAC}, \theta, p_m, p_0, T_0) = m_{ac}(p_m, \omega_e) \cdot \frac{n \cdot \omega_e}{4\pi} \tag{30}$$

The cylinder air charge (Fig.17) was estimated using the signal from the HEGO sensor and calibration data for the fuel injection system. With cylinder air charge known at every stoichiometric fuel conversion efficiency data point of Fig.19, (30) can be solved for the mean manifold pressure as a function of throttle angle, idle air duty cycle, environmental conditions and engine speed.

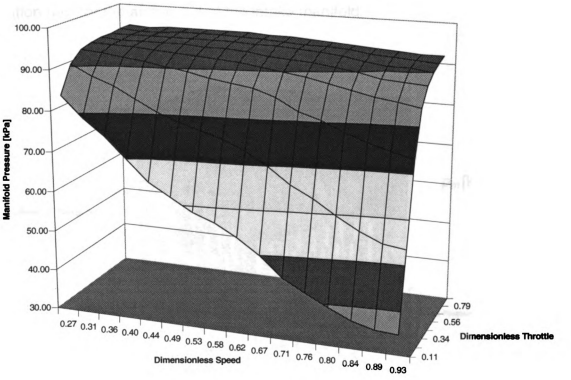

Fig.21: Measured Mean Manifold Pressure, 1995 1.9 liter Ford Escort without Air Filter, p_0 = 97.1 kPa, T_0 = 24.5 °C

Models for the idle air valve and the throttle valve were not generated. The mean manifold pressure (Fig.21) was obtained through direct measurement at the speed, throttle and idle air control conditions of the stoichiometric fuel

conversion efficiency data points (Fig19). The average output voltage of a manifold pressure sensor was recorded and related to the manifold pressure through sensor calibration.

The map (29) for the air charge as a function of manifold pressure and engine speed can be found combining mean manifold pressure (Fig.19) and cylinder air charge (Fig.17) and elimination of the throttle angle through linear interpolation between data points (Fig.21). This completes the model relation (28) for the airflow out of the intake manifold.

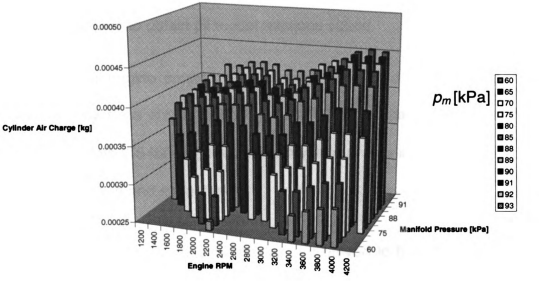

Fig.22: Cylinder Air Charge as a Function of Manifold Pressure and Engine RPM, 1.9 liter 1995 Ford Escort, using Fig.17 and Fig.21

CONCLUSION

A system's framework for the engine subsystems and their signal or power interactions was presented. Care was taken to obey causality when characterizing the interactions. Steady state mean value input-output relations for the different subsystems were derived based on dynamometer test data for the 1995 1.9 liter Ford Escort. Engine model control inputs are throttle angle, idle air control, fuel injector pulse width and spark advance. Engine output performance was formulated in terms of mechanical power or specific fuel consumption. Experimental procedures were proposed or references provided to obtain all model relations stated.

A test stand for engine control research was developed and its ability to generate steady state engine control models demonstrated. The Cosworth Intelligent Controls IC5460 Engine Control System ® was installed and used to vary fuel injection and spark timing.

All sensors and actuators were calibrated and proved to function reliably. It was observed that steady laminar flow calibration results for the mass airflow sensor could not be used in the running engine due to lack of accuracy. If the mass airflow sensor is used to drive future engine control algorithms, care must be taken to software compensate for mass airflow sensor systematic errors as a function of engine speed and engine load. A more precise

dynamic flow model for the mass airflow sensor may yield better insight into its complex flow dynamics.

The engine model presented was identified except for the following parts. The dependency of the Minimum Spark Advance for Best Timing on cylinder air charge and engine speed needs to be verified through direct measurement. Steady flow models for the throttle body and the idle air valve need to be generated. To measure the airflow contribution of the idle air valve, a series of tests without idle air valve could be run and air charge compared to those from tests with idle air valve. Airflow through the throttle and through the idle air valve are then related to the environmental conditions, the mean manifold pressure, the idle air valve duty cycle and the throttle angle.

The map (15) for the stoichiometric fuel conversion efficiency as a function of manifold pressure and engine speed is found combining fuel conversion efficiency (Fig.19) and mean manifold pressure (Fig.21) and eliminating the throttle angle through linear interpolation between data points. This will complete the model for the *Indicated Work* block.

The modeling strategy and measurement procedures proposed are applicable to any port fuel-injected spark ignited internal combustion engine without exhaust gas recirculation. The procedure delivers mean value steady state relationships only. Due to its causal formulation, the model can be extended dynamically by inclusion of state equations for the *Intake Manifold*

(state p_m) and the *Mechanical Dynamics* (state ω_e). Model relations (1, 2, 15, 22, 27, 28, 29) were all formulated in terms of the inputs and the state variables of the dynamic model. The relations stay valid, even under dynamic changes in inputs, mean manifold pressure or engine speed.

APPENDICES

APPENDIX A

ENGINE-DYNAMOMETER SETUP

A.1 Dynamometer Specifications

A.1.1 General Electric DC Electric Dynamometer

Type: TLC-2464H, Form: FN

Model: 26G230

Voltage: 250 volt

Current: 550 A

Generator mode: absorbs up to 200 hp

Motor mode: delivers up to 150 hp

Speed: 2500-6000 RPM

Load cell lever arm: 18.007″ = 1.5006 ft

Checking lever arm: 27.011″ = 2.2509 ft

A.1.2 Load Cell (south side)

BLH Electronics, Inc, Waltham, Massachusetts

Type: U3G1C, Serial # 95910

Capacity: 1000 lbf

Bi-directional load capability: (-) torque reading when loaded in compression

(+) torque reading when loaded in extension

A.1.3 Variable Reluctance Speed Sensor (shaft west end)

Amphenol 165-34 8703

Type: ring gear, 60 teeth/revolution

Terminal identification:

A: +12 volt DC

B: Direction output

C: Ground

D: Frequency output

E: Frequency output

A.2 Dynamometer Sensor and Actuator Calibration

A.2.1 Load Cell/Torque Display Calibration

Weight applied at checking lever arm: 9.8 lbf

Corresponding actual torque: 9.8 lb x 2.2509 ft = 22.1 ftlb

South end lever arm torque reading: -25.2 ftlb compression

North end lever arm torque reading: 17.8 ftlb extension

Torque offset: (-25.2+17.8)/2 = -3.7 ftlb

⇒ Apply counterweight on North end lever

Required counterweight: 3.7/2.2509 = 1.64 lbf

South end lever arm torque reading with counterweight: -21.4 ftlb

North end lever arm torque reading with counterweight: 21.0 ftlb

Comparison with actual torque (22.1 ftlb) ⇒ torque display accuracy ± 1 ftlb

A.2.2 Dynamometer RPM Display Calibration

Calibration reference: BEI 360 pulses/revolution crankshaft encoder together with the Cosworth IC5460 display.

Calibration results are shown in Table A.1 and Fig. A.1.

Table A.1: Dynamometer RPM Display Calibration

Dynamometer Display RPM	Encoder RPM
810	800
1009	1000
1211	1200
1414	1400
1616	1600
1818	1800
2022	2000
2220	2200
2425	2400
2627	2600
2828	2800
3030	3000
3236	3200
3434	3400
3639	3600
3837	3800
4038	4000

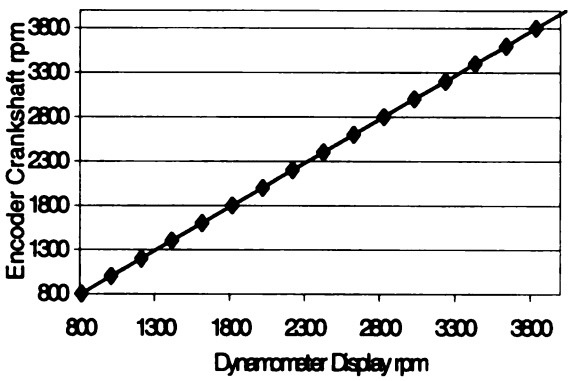

Fig. A.1: Dynamometer RPM Calibration

A.2.3 Dynamometer Throttle Actuator

The dynamometer throttle actuator is shown in Fig. A.2. The throttle cable is attached to the actuator lever arm in such way that full actuation range corresponds to the throttle opening from 0° to 90°. Attach the cable to the

hole in the actuator lever arm that closely corresponds to full throttle opening range.

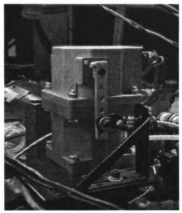

Fig. A.2: Throttle Actuator

Table A.2: Dynamometer Throttle Position Display Calibration

Dynamometer Throttle Display Reading	TPS Angle [deg]
4.8	0
145	5
176	10
227	15
258	20
296	25
349	30
381	35
430	40
474	45
503	50
548	55
588	60
634	65
680	70
716	75
766	80
804	85
874	89.2

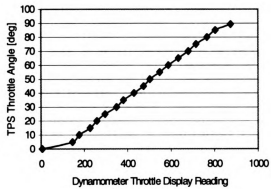

Fig. A.3: Dynamometer Throttle Position Calibration

A.2.4 Dynamometer Throttle Position Display Calibration

Calibration reference: Ford throttle position sensor (TPS) type F2CF-9B989AA, L1 2H05 AH together with Cosworth IC 5460 display.

Calibration results are shown in Table A.2 and Fig. A.3.

A.3 Engine-Dynamometer Coupling Design

Design requirements:

- overall coupling length as small as possible
- engine de-coupling from the dynamometer must be possible without moving the engine, such that engine aligmnent is maintained after de-coupling.
- critical torque transmission: 100 hp at 3500 RPM
- required speed range: 800-5000 RPM
- coupling must withstand crankshaft torsional vibrations due to multi-cylinder discontinuous crankshaft torque production

For design procedure, please refer to the Dodge ® Engineering Catalog [Reliance Electric Industrial Company, pp. C2-3 to C2-31, D1-5 to D1-9, 1993]. The design procedure is outlined on page C2-4.

Torque transmission requirement factor: hp x 100/RPM = 2.85

Safety factor (refer to p C1-4):

- driven unit: dynamometer ⇒ 1.0

- driver unit: 4-cylinder gasoline engine ⇒ 0.5

safety factor = $\sum$ = 1.5

Actual torque transmission requirement = safety factor x 2.85 = 4.27

PX80 on page C2-4 satisfies torque requirements, but the maximum coupling speed is only 3500 RPM ⇒ go to high speed and flywheel couplings pp. C2-22 to C2-29. A flywheel coupling mounts directly to the engine flywheel with the coupling body inside the engine belthousing. This allows reduction of the overall coupling length.

Coupling chosen: Paraflex Flywheel Coupling PH96, steel flange

- Maximum speed: 5230 RPM > 5000 RPM ⇒ OK
- Torque transmission capability factor: 4.5 > 4.27 ⇒ OK

Use of a taper lock bushing at the side of the coupling connecting to the coupling shaft, allows to disconnect the coupling shaft and slide into the belthousing without moving the engine.

Summary of the coupling parts:

- PX80: taper lock flange part # 010604
- PF96: bolt ring assembly part # 011248
- PH96: flexible element part # 011228

- taper lock bushing, bush # 2012, 1 3/8″ bore part # 117091

- shaft (engine side): diameter 1 3/8″ over 2″, keyseat 5/16″ x 5/32″

- nominal shaft dimensions: length 12″, diameter 1 ½″

The Paraflex flywheel coupling allows a limited degree of misalignment between the axes coupled (Fig. A.4). The engine alignment must then be well within the tolerances given.

Conclusion: the design reduces the coupling length outside the belthousing to 4″. Fig. A.5 shows a picture of the coupling as mounted inside the engine belthousing.

Maximum angular misalignment

Maximum parallel misalignment

Fig. A.4: Angular and Parallel Axis Misalignment

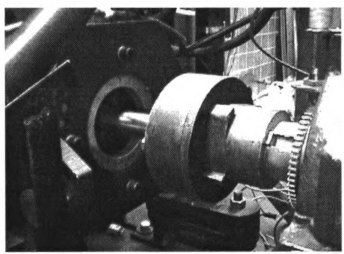

Fig. A.5: Engine-Dynamometer Coupling

A.4 Engine Specifications

1995 Ford Escort 1.9 liter, inline four-cylinder

A.4.1 Engine Block

Cylinder bore	3.23˝ = 8.204 cm
Stroke	3.46˝ = 8.788 cm
Displaced volume/cylinder	0.4646 dm^3
Compression ratio	9.1

A.4.2 Engine Cooling System

Coolant	50-70 % ethylene glycol, 50-30% water
Thermostat	195 ºF, Parts Master # 31399
Coolant pressure	12-15 psi

A.4.3 Fuel System

Injector pressure drop	40 psi
Pressure downstream fuel pump (running)	35-40 psi (not running), 30-45 psi
Injector type	saturation, 11-18 ohm
Injector flow rate	6.44 kg/hr
Injector offset	0.8 ms
Compatible injector serial # (part # 2-18076)	0280 150 907, 0280 150 937, 0280 150 938, 0280 150 941,

	FOSE-9F593-A5A,
	FOSE-9F593-A1A (currently on engine),
	FOSE-9F593-B1A, FOSE-9F593-B5A,
	FOSZ-A, F13Z-A, CM-4673, CM-4722

A.4.4 Ignition System

Firing order	1-3-4-2
Ignition principle	spark-ignited
Ignition configuration	2-coil electronic distributorless ignition
Compatible spark plugs	Champion 304 RS9YC, Autolite 5144
Spark wires	7 mm, double silicone core

For detailed engine dimensions and specifications, please refer to Ahlstrand [Ahlstrand, A., Haynes, J.H., 1996]. The engine control system is discussed in Appendix C.

A.5 Engine Bracket Design

The engine bracket must allow aligning the engine with the dynamometer shaft and attaching the engine to the dynamometer base plate. The existing front bracket and the attachment plate to the rear support pillar were modified for this purpose. Drawings of the new parts are found below (Fig A.6, Fig. A.7, Fig. A.9).

A.5.1 Front Bracket Base Plate

The front bracket base plate has two bolt slots for mounting the front bracket to the dynamometer base plate. Base plate dimensions are given in Fig. A.6.

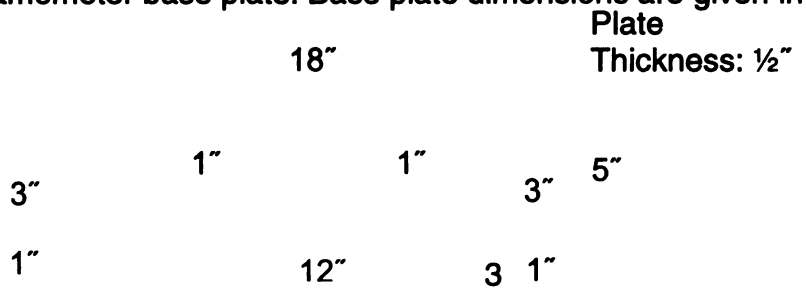

Fig. A.6: Front Bracket Base Plate

A.5.2 Front Bracket U-Profile Bridge

The front end of the engine is brought up to the height required for the dynamometer shaft and crankshaft to couple by means of a U-profile bridge. The bracket extensions of the belthousing mount onto the bridge. The bridge is welded onto the front bracket base plate. Bridge height is initially chosen 3/8″ too high. Height finishing and welding onto the bracket base plate is done only at the time of engine alignment. Final bridge dimensions then carefully compensate for alignment errors. The U-profile construction is shown in Fig. A.7.

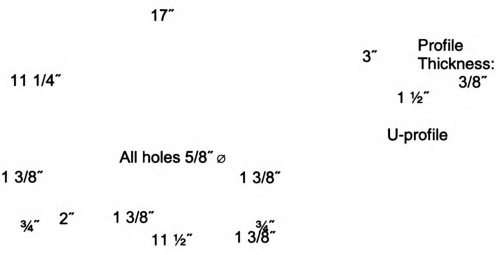

Fig. A.7: Front Bracket Bridge and U-profile

Fig. A.8 shows the engine supported by the front bracket.

Fig. A.8: Engine-Front Bracket Mounting

A.5.3 Rear Support Pillar Mounting Plate

The rear support pillar mounting plate is mounted onto the rear part of the engine block and suspended onto the support pillar.

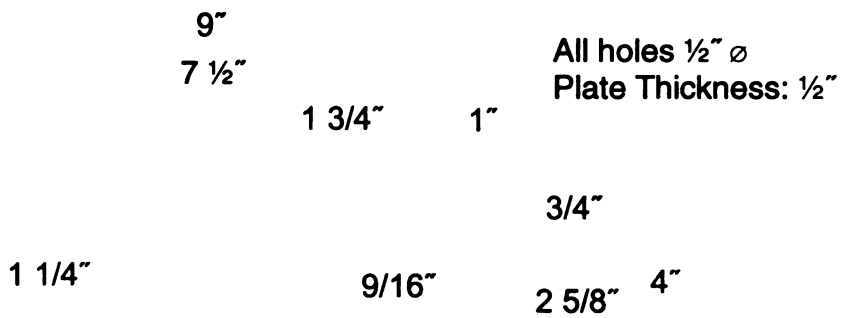

Fig. A.9: Rear Support Pillar Mounting Plate

After cutting and drilling, the plate is bend over an angle of 10 degrees (Fig. A.10).

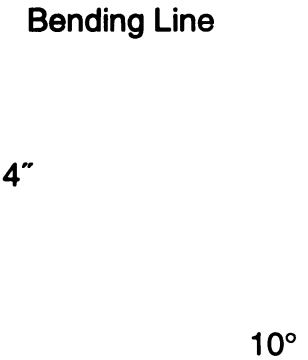

Fig. A.10: Rear Support Plate Bending

Fig. A.11 shows the engine suspended onto the rear support pillar.

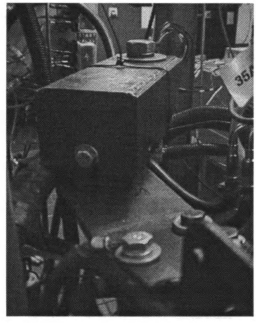

Fig. A.11: Engine-Rear Support Pillar Mounting

A.6 Engine Alignment

A bridge with pulley was built to facilitate engine alignment (Fig. A.12).

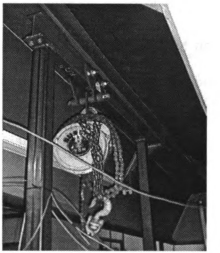

Fig. A.12: Bridge with Pulley

Six engine block degrees of freedom need to be checked during the alignment procedure: vertical translation, left-right translation, front-rear translation, front-rear tilting, lateral tilting and rotation about the vertical axis.

First, the unfinished front bracket is mounted onto the engine. Vertical translation is checked (engine crankshaft with respect to the position of the dynamometer shaft), as well as lateral tilting. Left and right pillars of the front bracket U-profile bridge (Fig. A.7) are finished following the errors measured. Finishing of the front bracket bridge fixes vertical translation of the coupling and lateral tilting. The front bracket base plate is now tightened to the dynamometer base plate and the finished front bridge is remounted to the engine.

Front-rear tilting is checked next: angular misalignment must be within the specifications of the coupling (Fig. A.4). The height of the rear support pillar is adjusted to compensate for angular misalignment.

The only degrees of freedom unfixed at this point are the planar degrees of freedom in the horizontal plane. Left-right translation and rotation about the vertical axis must satisfy the coupling specifications (Fig. A.4). All three planar degrees of freedom are fixed at once by

(1) marking the welding positions of the front bridge onto the front bracket base plate, as well as indicating the front bracket base plate position on the dynamometer base plate

(2) shifting the rear end support pillar in the horizontal plane.

The rear support pillar is tightened to the dynamometer base plate. The setup is taken apart again and the front bracket is now welded together. After alignment, coupling and dynamometer shafts are bolted together. Free rotation is checked by means of manually turning the coupling. Finally, the engine is motored at low speed for several minutes. If coupling shaft neither coupling feel warm, alignment is successful.

A.7 Engine Cooling System

The engine cooling system was modified. The engine coolant pump still drives the coolant circulation, but instead of using the engine radiator, the coolant is passed through a heat exchanger outside the building. A valve system is designed to allow easy draining of the coolant and to make it

possible to couple two different engines to the same heat exchanger. Fig. A.13 gives a picture of the valve system with the valves numbered for explanation.

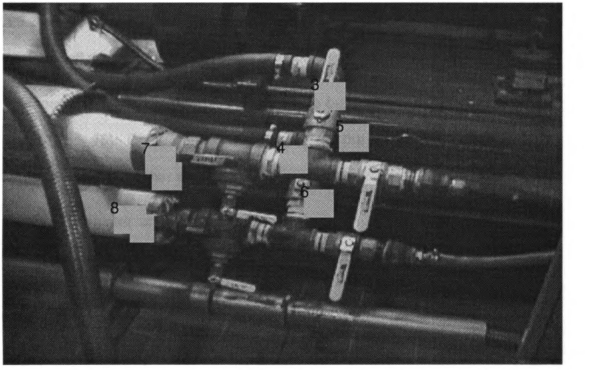

Fig. A.13: Coolant Valve System

Valves are open when the handle is parallel to the line. The arrows indicate direction of coolant circulation to the heat exchanger and the engines. Valves #1 and #2 shut off the lines to the heat exchanger. They are shut whenever draining or filling the engine block. In all other cases, these valves remain open to allow for circulation through the heat exchanger.

A.7.1 Heat Exchanger Switching between Two Engines

Engine access valves #3 and #4 are open when engine #1 is operational. In such case, valves #5 and #6 need to remain closed to prevent flow through

engine #2. Engine access valves #5 and #6 are open when engine #2 is operational. In such case, valves #3 and #4 need to remain closed to prevent flow through engine #1.

A.7.2 Coolant Draining Procedure

1. Shut off the valves #1 and #2 to the outside heat exchanger.
2. Open the access valves of the engine to be drained (either #3 and #4 or #5 and #6). Close the access valves of the other engine to prevent draining of the other engine.
3. Place canister under the draining valves #7 and #8. Open the draining valves and wait for the cooling system to drain.
4. Close the draining valves #7 and #8 after draining.

A.7.3 Coolant Refill Procedure

1. Shut off the valves #1 and #2 to the outside heat exchanger.
2. Make sure the draining valves #7 and #8 are shut.
3. Open the access valves of the engine to be refilled (both #3 and #4 or #5 and #6). Close the access valves of the other engine to prevent draining of the other engine.
4. Add coolant to the coolant reservoir mounted above the engine block (Fig. A.14) and wait for the air to vent.
5. Close the coolant reservoir and open the valves #1 and #2.

6. Motor the engine at low speed. Check whether there is flow in the cooling system (even in motoring conditions, the coolant hoses from the reservoir to the oil filter should be warm due to compression heat). If there is no flow, open the coolant reservoir carefully while motoring the engine and release the compressed air in the lines. When a bubbling sound is heard which indicates starting flow, immediately close the coolant reservoir.
7. Stop the engine and shut the valves #1 and #2.
8. Add coolant to the reservoir if necessary.
9. Reopen the valves #1 and #2 and fire the engine to allow for the engine block to heat up and for the thermostat to open.
10. Repeat steps 7 and 8.

A.7.4 Operating Conditions

Coolant temperature: 180-195 ºF

Coolant pressure: 12-15 psi.

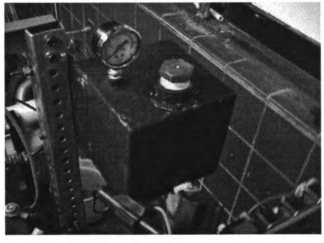

Fig. A.14: Coolant Reservoir

A.8 Exhaust System

An exhaust fan (Fig. A.15) outside the building sucks the exhaust gases out of the exhaust pipe and blows them into the chimney.

A.8.1 Fan Specifications

Baldor Industrial Motor, Single Phase

Cat: VL3513 Spec: 35C13-199 Ser: F398

Power: 1 ½ hp

Voltage: 115/208-250 volt

Current: 15/7.9-7.5 A

Speed: 3450 RPM

Frequency: 60 Hz

Rating: 400 AMB-CONT

Wiring: (low voltage) join wires 1-3-8, join wires 2-4-5. To reverse rotation, interchange connectors 5 and 8.

A.8.2 Heat Shielding

All exhaust components must be properly shielded and must ABSOLUTELY avoid contact with the coolant hoses, the coolant insulation or the spark wires. The exhaust manifold must be covered with a heat shield to protect the spark wires.

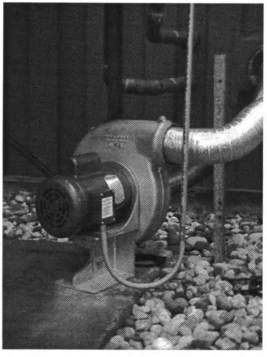

Fig. A.15: Exhaust Fan

APPENDIX B

DYNAMOMETER OPERATION

This appendix uses information from an earlier engine-dynamometer startup description [Fitzpatrick, T., 1995]. The document was modified when necessary to account for changes made to the engine-dynamometer setup.

B.1 Safety Checks

B.1.1 Fire Safety

1. Coolant lines may not touch the fuel lines, or any of the wires of the electronic control unit.
2. The fuel can ground clip must be grounded to engine ground and kept away from the battery.
3. No liquid fuel may be apparent on the ground near the battery, on the engine or on the dynamometer base plate, such as often occurs after working on the fuel injection system or after refill of the fuel can. In such case, turn on the ventilation tubes and let the fuel evaporate first before running the engine.
4. Spark wires may not touch the exhaust manifold.
5. All exhaust components must be properly heat shielded and avoid contact with the coolant lines, flammable objects or parts that can melt.
6. Fire extinguishers must be placed at both sides of the engine.

7. A manual emergency button near the dynamometer control box allows shut off of ignition and fuel supply to the engine. The emergency switching circuit is described in Appendix C.4
8. Engine overheating is prevented by an over-temperature relay, which shuts off both ignition and fuel supply in case of overheating (Appendix C.4).

B.1.2 Mechanical Safety

1. Every day of dynamometer testing, check whether the coupling bolts and taper lock nuts are tight.
2. Make sure hose clamps on all coolant hoses are tight.
3. Make sure there are no obstructions on the dynamometer or engine, such as rags, tools and cords.
4. Make sure sensor cables don't touch rotating parts and are kept away from spark wires.
5. Check whether Hall effect sensor mounting bracket is tight.
6. Make sure spark wires, fuel injectors and all sensors are properly connected.
7. Make sure no data acquisition or measurement equipment is located within the plane of the rotating coupling.

B.2 Pre-run Check and Running Preparation

1. Check engine oil level.

2. Check coolant level in the coolant reservoir above the engine (Fig. A.14). When doing this, make sure to close the valves to the heat exchanger.
3. Make sure the battery is charged (12-14.8 V).
4. Plug in the exhaust fan.
5. Turn on the ventilation tubes above the engine (switch with red-yellow-green lights is located in green box attached to Tom's office).
6. Connect the 12 V battery to the power cables from the engine control stand. Red is positive.
7. Connect fuel can to fuel system:
    A. Hose quick connectors are interchangeable
    B. Make sure fuel can ground clip is connected to the engine ground.
8. Make sure that the main valves for the cooling system are open, as well as the access valves to the engine being run (valve handles parallel to the pipe).
9. Turn on the fans for the heat exchanger. Switches are located on the wall directly above where the coolant pipes pass through.

B.3 Dynamometer Startup

Fig. B.1 and Fig. B.2 show the two main dynamometer electronic circuit parts: the DC drive, which contains the high voltage power electronics and the dynamometer control cabinet, which contains the control electronics.

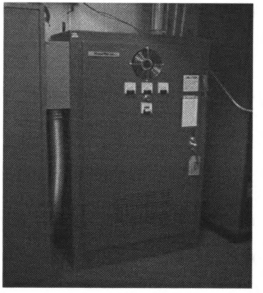

Fig. B.1: Dynamometer DC Drive

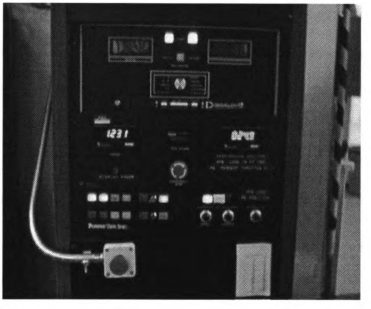

Fig. B.2: Dynamometer Control Panel

1. Turn on the main power to the dynamometer (the switch is located on the 480 V bus way).

2. Make sure that the EMERGENCY STOP buttons on the DC drive and on the control panel are pulled out.

3. Turn on the DC drive (lift handle into the upward position). The fan inside the DC drive cabinet should go on.

4. Turn on the display power by pushing the left red button in the middle of the control panel.

* The steps 5-7 require a key to operate the switch.

5. Turning direction of the dynamometer: engines turn counterclockwise when looking from the front end (the end of the crankshaft coupling to the dynamometer) to the rear end. Motoring the engine in the wrong direction severely damages the oil pump. Therefor: CAREFULLY CHECK ON THE TURNING DIRECTION BEFORE PROCEEDING WITH A TESTRUN. Turning the key in between the "forward" and "reverse" knobs on the control panel sets the turning direction. TO RUN AN ENGINE ON THE WEST END: PUT DYNAMOMETER IN "REVERSE" ROTATION (switch should light yellow), TO RUN AN ENGINE ON THE EAST END: PUT DYNAMOMETER IN "FORWARD" ROTATION (switch should light red).

6. Make sure the controller is set on "Manual", not "Auto". The switch should light yellow.

7. Make sure the controller is set on "Speed", not "Current". The dynamometer is not set up to run in the "Current" mode. The switch should light yellow.

8. With the "Fault Reset" button illuminated, push the "Drive Power On" switch. This will turn on the oil pump and the two fans at the West end of

the dynamometer. The "Drive Power On" switch should light green. The light of the turning direction switch will go on, as well as the lights of the "Manual" and "Speed" switches.

If the "Fault Reset" button is initially not illuminated, the "Drive Power On" will not react. In such case: open the DC power drive cabinet with a screwdriver. DO NOT TOUCH ANY OF THE ELECTRONIC CIRCUITRY! Look for the display through the hole in the gray box at the bottom of the power electronics. The display should show "P00", which is the reset location of the control program. If "P00" doesn't show: push the blue button to the left of the display BY HAND (Fig. B.3). Keep pushing the blue button until "P00" appears on the display. Close the DC drive cabinet. The "Fault Reset" button on the control panel should now illuminate. Push the "Drive Power On" switch and the system should react as stated above.

If the system still doesn't react: turn the DC drive power off as well as the main power to the dynamometer. Check the fuses inside the DC drive power cabinet. Replace bad fuses and repeat steps 1 through 8.

9. If the dynamometer has not been run for two weeks or more, stop at this step for ½ hour to allow lubrication.

10. Press the "Fault Reset" switch. The "Fault Reset" switch light should now be off. The "Fault Reset" button resets the speed scale to zero. IF THE FAULT RESET IS NOT PRESSED BEFORE PUSHING THE "RUN" BUTTON, THE SPEED SCALE HAS AN OFFSET AND THE DYNO MAY

START TO ROTATE IN THE OPPOSITE DIRECTION AS EXPECTED, EVEN WHEN ZERO SPEED IS INDICATED.

11. Make certain the "Throttle" and "Speed" turning knobs are turned all the way counter-clockwise.

12. Turn on the throttle controller by pushing the two yellow buttons on top of the control panel. Both yellow buttons should light.

13. Depress white "XFB" or "P/E" button on the throttle controller. These buttons define the dynamometer control mode (see below). WHILE RUNNING, THE CONTROL MODE MAY NEVER BE CHANGED! THE DYNO IS NOT SET UP TO RUN IN ANY OTHER CONTROL MODES THAN THE ONES MENTIONED: DO NOT PUSH ANY OTHER WHITE BUTTONS OR SEVERE DAMAGE MAY OCCUR.

14. Turn on fuel pump and engine ignition. The procedures for engine firing and shutdown are discussed in Appendix C.7 for operation with the Ford Control System.

15. For a run in "P/E" mode: with the silver knob on "SP" (set point), turn the "Throttle" knob until it shows about 150 (or 15% throttle). In "XFB" mode: with the silver knob on "SP" (set point), turn the "Throttle" knob to set the desired load torque at idle (in ftlb, e.g. 60-70 ftlb for the Ford Engine).

16. Press the "Run" switch. The switch should light green. The main fan of the DC drive cabinet should go on.

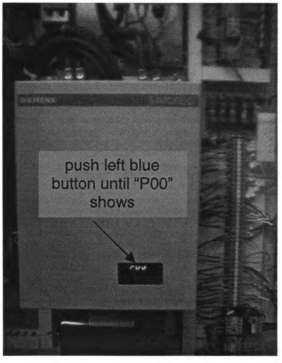

Fig. B.3: Dynamometer DC Drive Display Location

17. Turn the "Speed" knob until the engine is motored at 1200 RPM (high idle). IT IS NOT ADVISABLE TO RUN THE DYNAMOMETER AT LOWER SPEEDS.

A scheme of the startup settings is given in Table B.1.

Table B.1: Dynamometer Startup Sequence

No.	SETTING LABEL	WEST DYNO	EAST DYNO
1.	EMERGENCY STOP	PULLED OUT	PULLED OUT
2.	MAIN POWER	ON	ON
3.	DC DRIVE	ON (handle up)	ON (handle up)
4.	DISPLAY	ON (red button)	ON (red button)
5.	ROTATION	REVERSE (yellow)	FORWARD (red)
6.	CONTROLLER	MANUAL (yellow)	MANUAL (yellow)
		SPEED (yellow)	SPEED (yellow)
7.	DRIVE POWER	ON (green)	ON (green)
8.	FAULT RESET	yellow light off	yellow light off
9.	THROTTLE KNOB	totally left	
10	SPEED KNOB	totally left	totally left
11.	THROTTLE CONTROLLER	ON (two yellow lights)	
12.	CONTROL MODE	P/E PUSHED IN	P/E PUSHED IN
13.	SET POINT	THROTTLE TO 150	
14.	RUN	ON (green)	ON (green)
15.	SPEED	1200 RPM	800 RPM

B.4 Dynamometer Control System

B.4.1 Control Display

The "RPM" part of the display window (red L.E.D. display on the left) always shows engine RPM. Calibration of the speed display is given in Appendix A.2.

The "performance knob" (the silver knob on the Throttle Controller) selects what system is monitored. The "performance monitor" (red L.E.D. display on the right) displays the value of the selection of the "Performance Knob": either torque or throttle. Calibration of the throttle display and torque display is given in appendix A.2.

NOTE: pay careful attention to the units! These are NOT displayed, however they DO change depending on the position of the "Performance Knob".

B.4.2 External Feedback Control Mode

Throttle controller white push button in "XFB". In this mode, you set the speed that the engine will run at, as well as the torque the engine is required to produce. Remark that this sets a requirement for engine power at the given speed. In this mode, the dynamometer is given control over the throttle actuation: the throttle will automatically open or close to try to achieve the required power setting at the RPM given. (i.e. the operator defines RPM and torque and throttle position is the variable).

The "Performance Knob" has the following usable settings in this mode:

"XFB" = External Feedback. This is the actual reading from the load cell in **foot-pounds**. This is the torque that the engine is actually producing.

"POSITION" = **percent throttle x 0.1**

"SP" = Torque Set Point in **foot-pounds**. This is where you set the load that the dynamometer will hold against the engine. To provide the engine from stalling: setting the load at a value greater than the engine can attain at the RPM given, will cause the throttle to fully open (WOT) in an attempt to reach the level given. Use the "Throttle" knob to adjust the set point.

"FB" = Feedback from the load cell in foot-pounds. This should be the same as "XFB"

B.4.3 Position/Excitation Control Mode

Throttle controller white push button in "P/E". In this mode, you set the speed that the engine will run at, as well as the throttle position. In this mode, the dynamometer will automatically adjust the load the engine sees to achieve those settings (i.e. the operator defines RPM and throttle and load torque is the variable).

Note: The dynamometer is only set up to use the "Position" function. Attempting to use "Excitation" will cause SEVERE DAMAGE to the

dynamometer and its components! Therefore, never push the red "Excitation" button on the throttle controller part of the control panel.

The "Performance Knob" has the following usable settings in this mode:

"XFB" = External Feedback. This is the actual reading from the load cell in foot-pounds. This is the torque that the engine is actually producing.

"POSITION" = **percent throttle x 0.1**

"SP" = Throttle Set Point in **percent throttle x 0.1**. This is where you set the throttle position that the engine will run at. To dynamometer will automatically adjust the load against the engine to maintain these settings. Use the "Throttle" knob to adjust the set point.

"FB" = Feedback from throttle actuator. This should be the same as "POSITION".

NOTE: IF THE DYNAMOMETER IS RUNNING IN "XFB" OR "P/E" AND SWITCHED TO THE OTHER SETTING, SEVERE LOADS MAY BE APPLIED OR REMOVED. For instance: in "XFB" the "SP" may be set to 80 (foot-pounds), but when switched to "P/E" the system reads the "SP" as 80 x 0.1 = 8 % throttle. This can cause quite a shock.

B.4.4 Loading the Engine in "XFB" Mode

1. Use the "Speed" knob to set desired RPM. The engine will always remain at that RPM, either motoring or absorbing.

2. To determine a throttle position required for a given load: set the "Performance Knob" to "SP", then specify the desired torque load using the knob labeled "Throttle". The dynamometer will automatically load the engine to the torque level specified while opening the throttle to maintain the RPM set previously. Switch the "Performance Knob" to "Position". This will display the throttle position required to produce the specified torque.

3. To determine the torque for a given throttle position: cannot be done in the "XFB" mode.

B.4.5 Loading the Engine in " P/E" Mode (measurement of Torque-speed Curves)

1. Use the "Speed" knob to set desired RPM. The engine will always remain at that RPM, either motoring or absorbing.

2. To determine engine brake torque for a given throttle: set the "Performance Knob" to "SP", then specify the desired throttle position using the knob labeled "Throttle". The dynamometer will automatically load the engine to maintain the RPM under the specified throttle position. Switch the "Performance Knob" to "XFB". This will display the torque produced at the throttle position specified.

3. To determine the throttle position required for a given load: cannot be done in the "P/E" mode.

B.5 Dynamometer Shutdown

1. Shut down the engine. Procedures for engine shutdown are given in Appendix C.7 for operation with the Ford Control.
2. Turn down the "Speed" knob until the dynamometer has stopped. While approaching zero speed, be careful not to turn the dynamometer into reverse direction (this may occur due to shifting of the zero speed set point during the test run)
3. Press the "Stop" switch below the "Run" switch. The main fan of the DC drive cabinet shuts off.
4. Turn off the throttle controller by pushing the two yellow buttons on top of the control panel.
5. Press the "Drive Power Off" switch below the "Drive Power On" switch.
6. Turn off the display power by pushing the left red button.
7. Turn off the DC drive by pulling down the handle.
8. Turn off the main power to the dynamometer, located on the 480 V bus
9. Turn off the fans for the heat exchanger.
10. It is advisable to let the exhaust fan as well as the ventilation tubes on for a couple minutes to allow exhaust gases and heat to be removed. Then unplug the exhaust fan and turn off the ventilation tubes.
11. Disconnect the cables from the battery.
12. Disconnect the fuel can and store it in the "flammables" cabinet.

Table B.2: Dynamometer Shutdown Sequence

No.	SETTING LABEL	WEST DYNO	EAST DYNO
1.	SPEED	1200 RPM	800 RPM
2.	SET POINT	THROTTLE TO 150	
3.	IGNITION	OFF	OFF
4.	SPEED KNOB	totally left	totally left
5.	THROTTLE KNOB	totally left	
6.	STOP	push red switch	push red switch
7.	THROTTLE CONTROLLER	OFF (two yellow lights off)	
8.	DRIVE POWER	OFF (red)	OFF (red)
9.	DISPLAY	OFF (red button)	OFF (red button)
10.	DC DRIVE	OFF (handle down)	OFF (handle down)
11.	MAIN POWER	OFF	OFF

APPENDIX C

ENGINE OPERATION USING THE ELECTRONIC ENGINE CONTROL MODULE FROM FORD

C.1 Functional Overview

The electronic engine control module sets ignition and fuel injection timing over the entire speed-load operating range of the engine, as well as the duty cycle of the idle air control (IAC) valve. Control algorithms for ignition and fuel injection are based on static mapping information with additional trimming routines for exhaust gas oxygen (EGO) feedback and cold start enrichment.

Camshaft and crankshaft position sensors provide triggering information for ignition and fuel injection timing. Throttle position sensor (TPS) and mass airflow (MAF) sensor provide information on engine load. The exhaust pipe contains a heated exhaust gas oxygen (HEGO) sensor for use in the EGO feedback fuel injection trimming. The cooling hose leaving the oil pump contains the engine coolant temperature (ECT) sensor used during startup. The intake system contains an air charge temperature (ACT) sensor used for fuel injection trimming. It is remarked that the ECT and ACT configurations were changed with respect to the original engine setup. Although the production engine is equipped with an exhaust gas recirculation (EGR) valve, the engine on the dynamometer test bed doesn't have EGR installed.

Additional analog displays and gauges provide oil pressure, coolant temperature, battery voltage, ignition current, coolant pressure and fuel pressure for quick checking during operation.

The engine is equipped with a multi-point sequential port fuel injection system and a dual coil electronic distributorless ignition system (EDIS). The engine control system consists of the control module, a breakout box for monitoring control signals, an operator panel with manual switches and the emergency switch below the dynamometer control panel.

Limited information was available on the Ford production control system. Although not complete, the following sections contain the information provided by Ford as well as additional data extracted from the engine control system through dynamometer tests. Also included are wiring diagrams, interface characterization (if available) and calibration data for sensors and actuators.

C.2 Sensors

The sensors provide input signals to the electronic control module and the electronic distributorless ignition system.

C.2.1 Crankshaft Position Sensor (Fig. C.1)

Part #: Motorcraft # FOEE-80315-A2B

Principle: Variable Reluctance Sensor

Features: 36 teeth, one tooth missing

Measured variables: engine *RPM*, crank angle, crank angle reference

Function: - provide degree-based trigger signal for ignition and fuel injection

- provide *RPM* as mapping input to the EEC

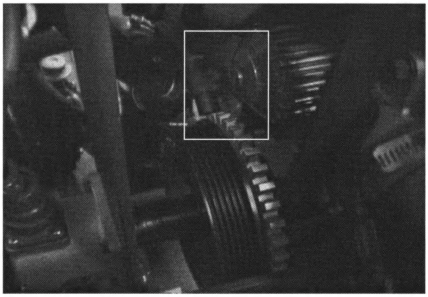

Fig. C.1: Crankshaft Position Sensor

C.2.2 Camshaft Position Sensor (Fig. C.2)

Part #: Motorcraft # FOEE-68288-A1A

Principle: undetermined

Measured variable: camshaft reference position

Function: provide reference pulse for the sequential fuel injection system. Remark that the dual coil ignition system doesn't need a cam reference since spark fires during both exhaust and compression strokes.

Fig. C.2: Camshaft Position Sensor (Located behind the Intake Manifold)

C.2.3 Throttle Position Sensor (Fig. C.3)

Part #: Motorcraft # F2CF-9B989-AA

Principle: rotary potentiometer

Measured variable: throttle position

Function: provide throttle position as mapping input to the EEC

Terminal identification:

A: Ground

B: Signal, low at closed throttle – high at wide-open throttle

C: +5 volt DC

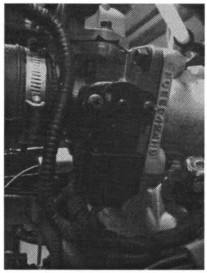

Fig. C.3: Throttle Position Sensor

The overall resistance (terminal A to terminal C) equals 3.48 kΩ. The resistance between terminals A and B varies linearly as a function of throttle angle (Fig. C.4) from 3.33 kΩ at closed throttle ($\theta = 0°$) to 0.73 kΩ at WOT ($\theta = 88.9°$). For Fig. C.4, it was assumed that in between closed throttle and WOT the throttle resistance varies linearly.

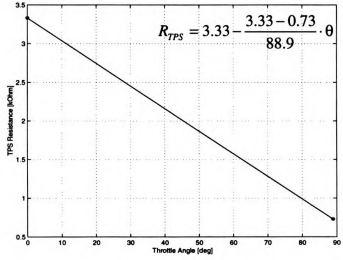

Fig. C.4: TPS Resistance

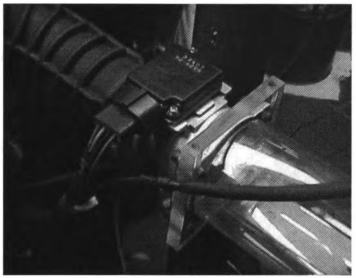

Fig. C.5: Mass Airflow Sensor

C.2.4 Mass Airflow Sensor (Fig. C.5)

Part #:'94-'95 engine models: Motorcraft # F37Z-12B579-A or F37Z-12B579-F

'91-'93 engine models: Motorcraft # F0CZ-12B579-A

IT IS UNCERTAIN WHETHER THE SENSOR ON THE ENGINE IS COMPATIBLE WITH THE ENGINE CONTROL SYSTEM. The sensor installed on the engine has the following part # which is different from the ones mentioned: FOCF-12B579-A. Calibration data given is for the FOCF-12B579-A model only.

Principle: hot wire anemometer in Wheatstone bridge

Measured variable: total mass airflow in the intake (= throttle flow + IAC valve flow)

Function: provide mass airflow as mapping input to the fuel section of the EEC

Terminal identification:

A: +12 volt DC (V_{ref}), battery supply

B: Ground

C: Signal (-)

D: Signal (+)

Table C.1: Mass Airflow Calibration (Sensor FOCF-12B579-A)

$\dot{m}$ [kg/hr]	V/V_{ref}
55.56	0.147
63.70	0.173
69.63	0.179
75.80	0.187
79.38	0.194
83.84	0.199
87.41	0.202
97.51	0.212
103.86	0.220
119.14	0.229
128.03	0.234
136.92	0.234
142.00	0.235
145.81	0.236
154.03	0.244
161.49	0.253
172.10	0.258
183.39	0.267
196.29	0.275
205.97	0.288
224.05	0.295
245.51	0.303
259.17	0.311
266.98	0.317

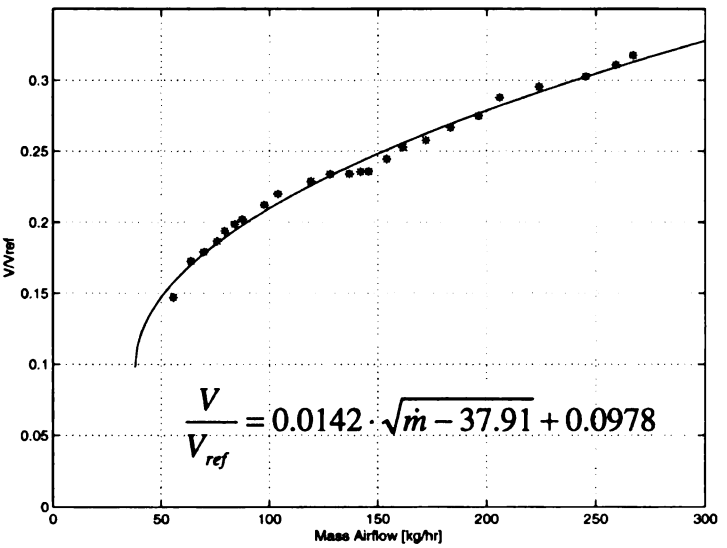

Fig. C.6: Mass Airflow Calibration (Sensor FOCF-12B579-A)

The voltage-airflow input-output relations of the mass airflow sensor were determined by running the sensor in the intake in series with the Hitachi/Ford sensor #ES-E8ZF-12B579-AA as a reference. The Hitachi/Ford sensor has known voltage-airflow characteristics. During calibration, the reference sensor was powered off a steady 12-volt voltage supply, whereas the calibrated sensor was powered off the car battery. Changes in the battery voltage V_{ref} during the test run were recorded and compensated for by calculating sensor output voltage as a ratio to the battery voltage V_{ref}. NOTE THAT CALIBRATION RESULTS ARE ONLY VALID IF THE VOLTAGE-AIRFLOW CHARACTE-RISTICS FOR THE HITACHI/FORD SENSOR WERE ACCURATE. Calibration results are shown in Fig. C.6 and Table C.1.

C.2.5 HEGO Sensor (Fig. C.7)

Part #: not available

Principle: oxygen driven voltage difference across ZrO_2 material

Features: sensor contains heating resistance, powered off the car battery

Measured variable: exhaust gas oxygen content

Function: provide relative A/F ratio information to the fuel section of the EEC

Terminal identification (refer to Fig. C.8):

A: +12 volt DC, battery supply (white wire)

B: ground (white wire)

C: signal (black wire)

The sensor signal is activated only after the sensor reaches operating temperature (above 300 °C). The sensor switches between high and low voltages depending on the relative A/F ratio λ of the exhaust gases. The switching voltage levels depend on the operating temperature. For the engine block operating above 195 °F, rich mixture (λ<1) corresponds to a sensor voltage > 800 mV and lean mixture (λ>1) corresponds to a sensor voltage < 70 mV.

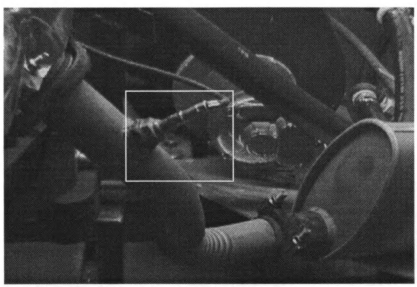

Fig. C.7: HEGO Sensor

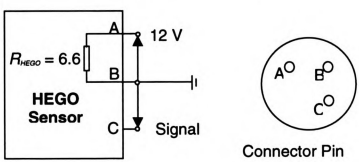

Fig. C.8: HEGO Terminal Identification

C.2.6 Air Charge Temperature (ACT) Sensor

Part #: Motorcraft # FOSF-9F472-AA

Principle: temperature dependent resistance, thermistor

Measured variable: intake air temperature

Function: provide intake air temperature information to the fuel section of the EEC

Terminal identification: 5 volt DC power and ground

The intake system has been modified with respect to the production engine. The ACT sensor is threaded into a transparent flow straightener in the intake (Fig. C.9). Change of sensor resistance with temperature is given in Fig. C.10 and Table C.2.

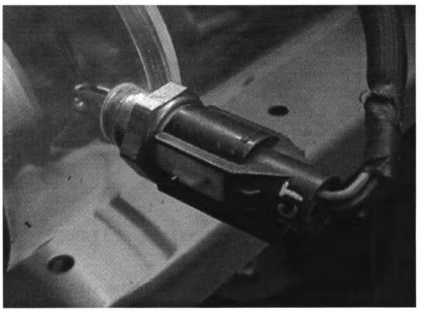

Fig. C.9: Air Charge Temperature Sensor

Table C.2: ACT Sensor Calibration (Sensor F2ZF-12A697-AA)

T_{ACT} [°C]	R_{ACT} [kΩ]
-20	269
-10	155.138
0	92.553
10	56.962
20	36.077
30	23.459
40	15.63
50	10.65
60	7.409
70	5.253
80	3.792

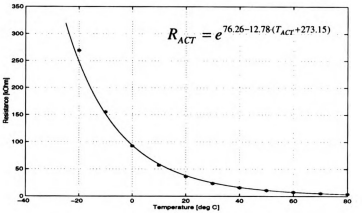

Fig. C.10: ACT Sensor Calibration (Sensor F2ZF-12A697-AA)

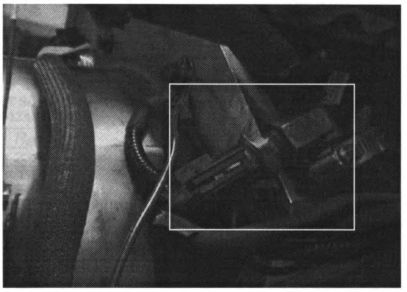

Fig. C.11: Engine Coolant Temperature Sensor

C.2.7 Engine Coolant Temperature (ECT) Sensor (Fig. C.11)

Part #: Motorcraft # E4AF-12A848-AA

Principle: temperature dependent resistance, thermistor

Measured variable: block coolant temperature

Function: - provide coolant temperature information to the fuel section of the EEC

- provide switch off signal to over temperature emergency relay

Terminal identification: 5 volt DC power and ground

The engine coolant system has been modified with respect to the production engine. The ECT sensor is threaded into the rubber hose connecting the oil pump to the thermostat housing (Fig. C.11). Change of sensor resistance with temperature is given in Fig. C.11 and Table C.3. Calibration was done with the OMEGA ® Engineering HH 81 digital thermometer (chromel-alumel thermocouple) as a reference.

Table C.3: ECT Sensor Calibration (Sensor E4AF-12A848-AA)

T_{ECT}	R_{ECT}
21.15	33.7
22.6	31.4
24.9	27.2
25.6	25.8
27	24.2
30	20.5
35	15.2
40	10.9
45.1	8.3
50	6.3
55	5.1
61.7	2.9

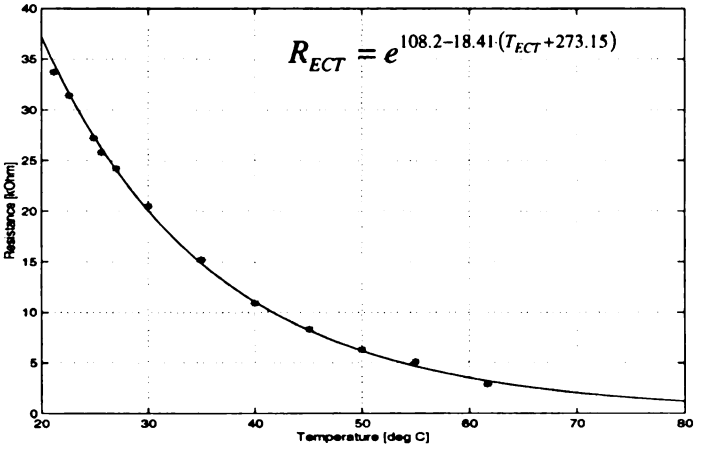

Fig. C.11: ECT Sensor Calibration (Sensor E4AF-12A848-AA)

C.3 Actuators

C.3.1 Fuel Injectors

Part #: Motorcraft #FOSE-9F593-A1A (gray body, labeled "A1" to "A4")

Part numbers of other compatible injectors are given in Appendix A.4. It is noted that the injectors on the spare engine (black body, labeled "B1" to "B4") were found compatible as well.

Principle: solenoid valve

Resistance: 14.8-15.0 Ω (saturation injector)

Mean Flow Rate: 6.44 kg/hr, Mean offset : 0.8 ms

Terminal identification: 12 volt DC battery supply and ground

In order to run routines for controlling A/F ratio, it is of crucial importance to know the exact flow rate of the injectors as well as their opening time (or offset). Flow rate determination was done in a flow bench test using the Cosworth IC5460 control system.

In a flow bench test, the injectors are fired a given number of times with a known pulse width. The total mass of fuel injected is weighted and divided by the number of injections to yield fuel mass per injection. The flow bench test is repeated for different values of the injector pulse width. A graph of mass per injection [gram] versus pulse width [ms] is generated and a linear least square fit obtained. The slope of the linear approximation is equal to the injector flow rate [kg/s]. The intersection of the curve with the pulse width axis is equal to the injector offset [ms].

Flow bench test results for the injectors (FOSE-9F593-A1A) on the engine are given in Fig. C.12. The injectors on the engine are labeled "A1" to "A4" with red ink corresponding to the plots of Fig. C.12. Flow bench results for the black body injectors on the spare engine (labeled "B1" to "B4") are not shown, but mean injector flow rate and mean injector offset were found to be the same as for the gray body injectors currently on the engine.

C.3.2 Idle Air Control (IAC) Valve (Fig. C.13)

Part #: Motorcraft # F2CE-9F715-AB

Principle: solenoid valve

Resistance: 10.0 Ω

Terminal identification: 6-12 volt variable duty cycle supply from the EEC

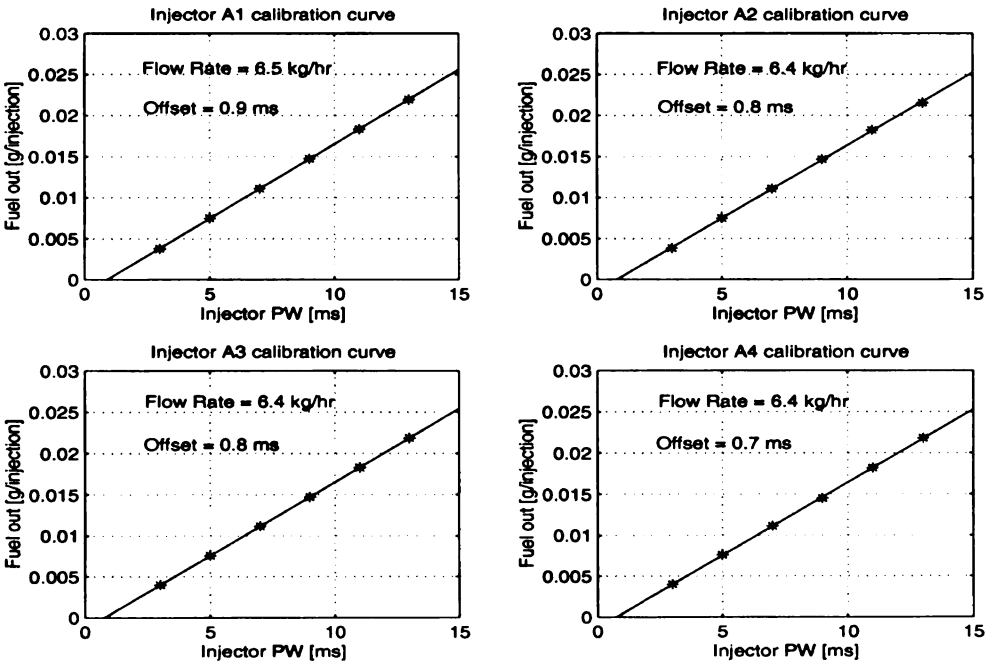

Fig. C.12: Flow Bench Test Results for Gray Body FOSE-9F593-A1A Fuel Injectors

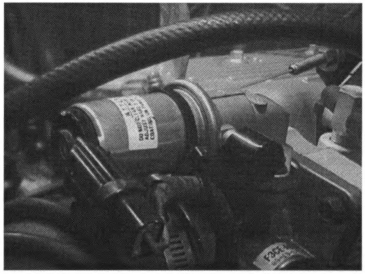

Fig. C.13: Idle Air Control Valve

C.4 Operator Panel Wiring Diagram and Emergency Switching

The operator panel forms the operator interface to the engine electronic system. It contains a bench of manually operated switches, relays for emergency operation and analog display windows. It also supplies battery power to the different engine subsystems and provides a common ground for all devices connected. Fig. C.14 shows a picture of the front of the operator panel.

Modifications to the panel were made: all dysfunctional wires and circuits were detached and the switching electronics changed with respect to the original setup in order to insure safety in case of emergency.

C.4.1 Switching electronics and relays

Manual switches on the panel are open when they are in the down position. There are six manual switches and one push button. From the left to the right: starter motor push button, ignition switch, fuel pump switch, unused switch, CAT PROTECT switch, PED switch and SPOUT CUTOFF switch. The upper row of

the front panel further contains three lights: ignition light (yellow), over temperature warning light (blue) and an unused red light. There are four numbered relays on the panel, two on the front and two on the back: over temperature relay (relay #1), ignition relay (relay #2), option relay (#3) and start relay (#4). In addition, there is one relay hanging at the backside. The emergency push button (red on yellow box) is located on the bottom portion of the dynamometer control panel.

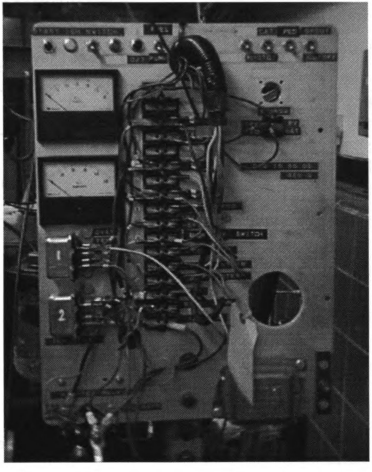

Fig. C.14: Front of the Operator Panel

The switching scheme for powering the engine electrical subsystems is given in Fig. C.15. The ignition switch activates main power to the fuel injectors, the

ignition module, the idle air control valve, the EEC and all sensor circuits. Remark that these functions are not separated: one cannot run ignition without applying power to the fuel injectors and the idle air valve. The fuel pump switch turns on battery voltage to the fuel pump. The fuel pump circuit is separated from the ignition circuit. This gives the operator the ability to motor the engine without supplying fuel to the fuel rail (engine not firing), while all other engine control electronics (fuel injectors, spark, idle air control valve and sensor I/O lines) are active as during normal operation.

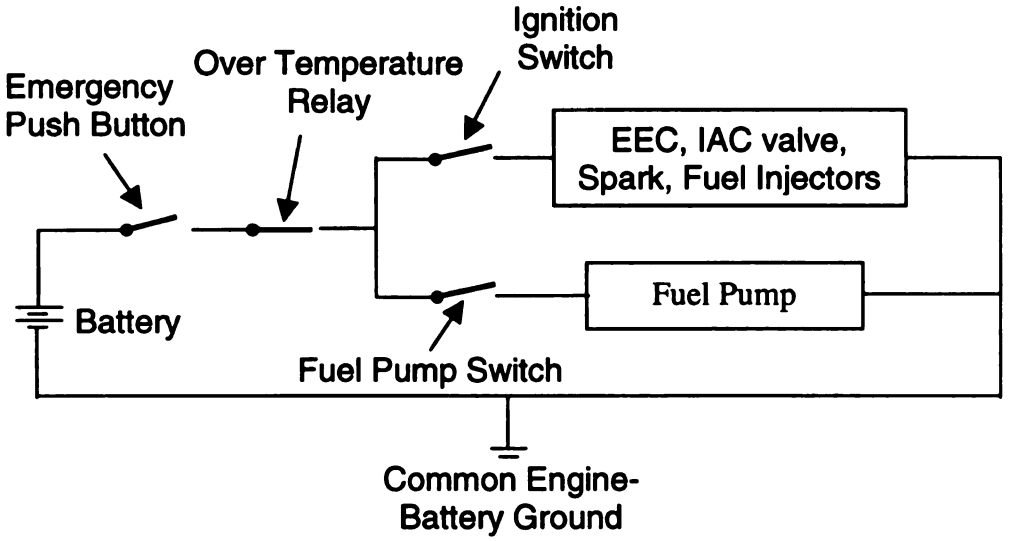

Fig. C.15: Switching Scheme for Power Supply to the Engine Electrical Subsystems

The over temperature relay and the emergency switch are placed in series with the fuel pump and ignition switch. Both will switch off ignition and fuel supply to the engine, as is required in an emergency shutdown. The emergency push button is closed (power supply) if pulled out, it is open (power shutdown) if pushed in.

The battery power supplied to the engine electronic systems and the fuel pump does not flow through the manually operated ignition and fuel pump switches. The ignition switch provides a signal to the ignition relay. It is the ignition relay that actually applies power to the engine electronic systems. The fuel pump switch provides a signal to the option relay. It is the option relay that actually applies power to the fuel pump. Battery power does however flow through the emergency push button and through the over temperature relay.

The implementation of the switching action of Fig. C.15 through manual switches, push buttons and relays is shown in Fig. C.16. The four main relays all have 5 terminals (labeled 1 to 5), with some terminals having two connecting pins. The main power supply to the relay comes through connector #5. Between connector #4 and connector #5 the relay has an internal coil. Outside the relay and also between connector #4 and connector #5 there's a resistor in parallel with the coil. The relay is then a switch, which connects terminals #1 and #3 if current flows through the coil. Terminal # 1 has battery power (12 volt) connected. Terminal #3 is connected to the circuit being powered by the relay.

Relay operation is then straightforward: if terminal line #4 is high, no current flows through the coil and the relay is not activated. Terminals #1 and # 3 don't connect, such that the circuit connected to terminal #3 is not powered. If terminal line #4 goes low, current flows through the coil and the relay is activated. Terminals #1 and #3 connect such that the circuit connected to terminal #3 is powered.

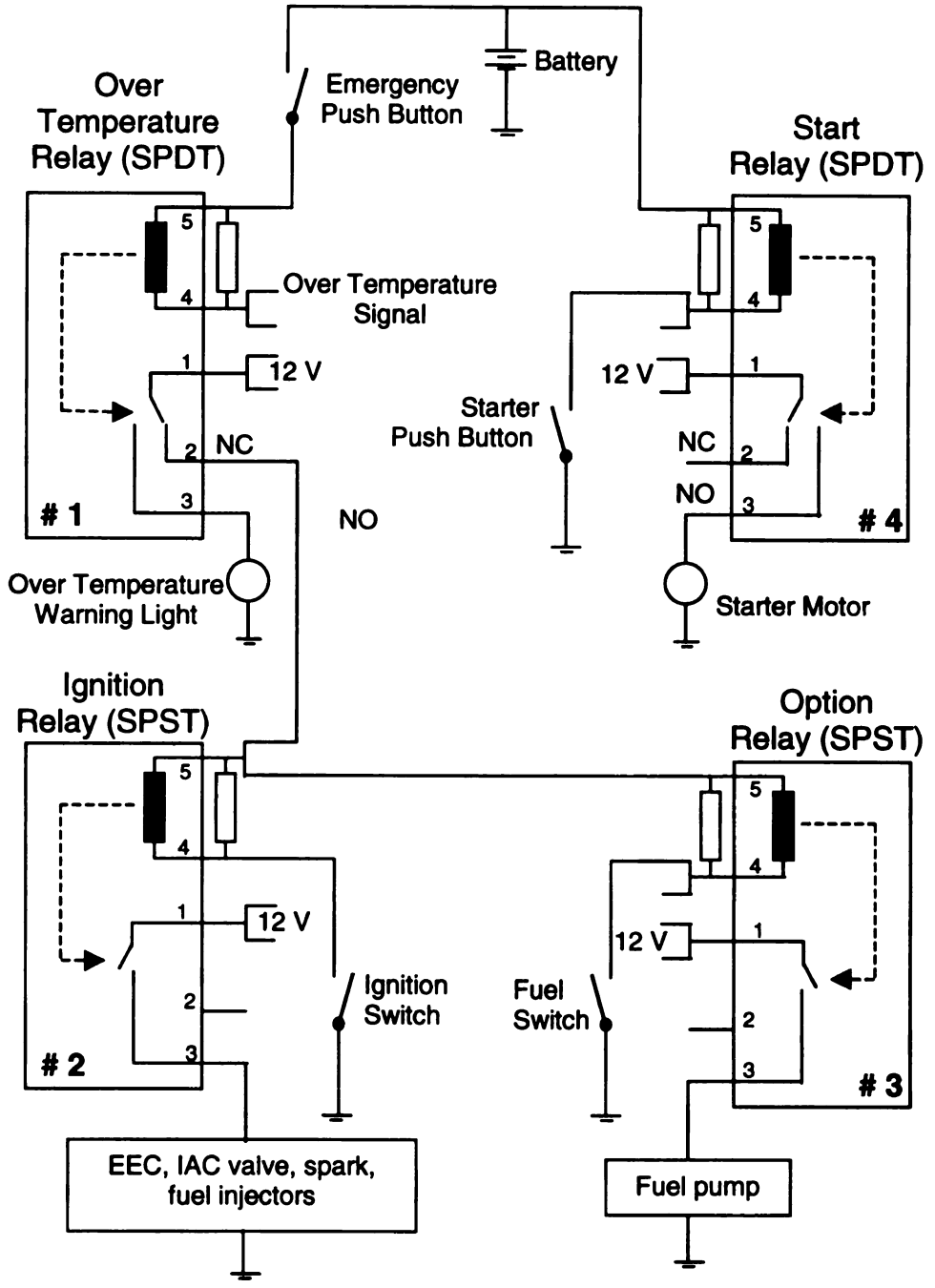

Fig. C.16: Operator Panel Switching Operation

Terminal #2 allows placing relays in series with one another. The over temperature relay (#1) and the start relay (#4) differ from the ignition relay (#2) and the option relay (#4), as far as terminal #2 is concerned. For relays #1 and #4, terminal #5 internally connects to terminal #2 if the relay is NOT active

(terminal #4 high). If the relay is active (terminal #4 low), terminal #5 and terminal #2 disconnect. For relays #2 and #3, there is no internal connection between terminal #2 and terminal #5 whatsoever, irrespective of whether the relay is activated or not. For relays #2 and #3, terminal #2 is then dysfunctional.

Switching operation can be read from Fig. C.16. If the emergency push button is pulled out, battery power is supplied to terminal #5 of the over temperature relay. As long as the temperature signal stays high (no over temperature), the over temperature relays passes through power to terminal #2 and by this to terminal #5 of both option relay and ignition relay. Turning the ignition switch on activates the engine control electronics because it brings terminal #4 of the ignition relay to ground. It will also turn on the yellow ignition light. Turning the fuel switch on activates the fuel pump, because it brings terminal #4 of the option relay to ground.

If over temperature occurs, the over temperature relay is activated, by this shutting off the power to both the ignition and the option relay. The fuel pump and the engine control electronics are shut down. In addition, the over temperature relay powers the blue warning light.

If the emergency button is pushed, no power is supplied any more to the option and the ignition relay, such that the fuel pump and the engine control electronics shut down.

The start relay is stand-alone with respect to the other electronics of the operator panel. Pushing the start button, which supplies power to the starter engine, activates the start relay. Remark that when operating the engine with the

dynamometer, the dynamometer itself is used for startup. The starter engine electronics were however left intact, such that a starter engine can still be hooked up to the operator panel.

Remark: the function of the hanging relay at the back of the operator panel is undetermined. This relay was most probably the original fuel pump relay (a function now taken by a different relay). Wiring of the hanging relay was left intact. It never activates the way it is currently wired. It is therefor dysfunctional, but it might have its use when wiring connections are changed appropriately.

C.4.2 Other Operator Panel Manual Switches

The SPOUT CUTOFF switch, when turned on, generates an interrupt to the engine controller. In response to the interrupt, the controller reduces spark advance with respect to the original engine control settings. The effect of the SPOUT CUTOFF switch on spark advance was not investigated in detail.

The function of the CAT PROTECT switch is undetermined. Turning it on applies battery power to the little black square box on the front panel (upper right corner). The function of the little black square box is undetermined.

The function of the PED switch (originally labeled "fuel pump") is uncertain. It interconnects with a troublesome electrical circuit, involving the hanging relay, the ignition switch, the little black square box on the front panel and a line connecting the operator panel to the EEC (probably an interrupt line). In order to power the line to the EEC, the hanging relay must activate, which never happens in the current setup.

When studying the operator panel, all switches with unknown functionality and circuits connected to these switches were left intact, IF these circuits somehow interconnect to the EEC or sensors. In all other cases, switches were disconnected and wires removed.

C.4.3 Analog Display Devices

The operator panel contains two analog display windows. A voltmeter (battery voltage) and an ampere meter (current drawn by the starter engine or the engine electronics). The current indicated on the ampere meter does not include the current drawn by the fuel pump or the distributorless ignition system.

An additional analog display with three windows is mounted against the steel pillar, which supports the pulley rail above the engine. The gauges monitor oil pressure (lower window) and coolant temperature (upper window). The middle window, which shows current, is not connected. The display lights are powered through the operator panel and light if the ignition switch is turned on.

Two pressure checking gauges were installed, one on top of the coolant reservoir and one in the line that connects the fuel pump to the fuel injector rail.

C.4.4 Wiring to the ECC, the EDIS and the Sensors

The wire connections between the operator panel, the ECC, the EDIS and the sensors were not studied in detail. Wiring diagrams for these connections are not yet available. Sensor interface characterization can be found in section C.2. Sensor input signals to the ECC as well as ECC output signals to the fuel

injectors and the IAC valve can be monitored off the ECC breakout box as explained in section C.5.

C.5 Breakout Box and Control Signal Monitoring

C.5.1 Breakout Box Pinout Chart

The breakout box of the Ford control system has 60 plug-in connectors for monitoring the controller's I/O signals on the oscilloscope (Fig. C.17). A chart with pin #, circuit # & wire color and signal definitions is given in Table C.4. The engine is not equipped with EGR, Canister Purge Solenoid, Air Conditioning, Clutch and Cooling Fan. Signal lines of the breakout box associated with these functions are marked "(n/a)" (not active). Signal lines which function are yet unidentified are marked with a question mark.

The chart was copied from an original fax from Ford titled "Connector Faces/Pinout Charts 150-10" and extended with additional information on the EEC I/O lines out of Ahlstrand (1996).

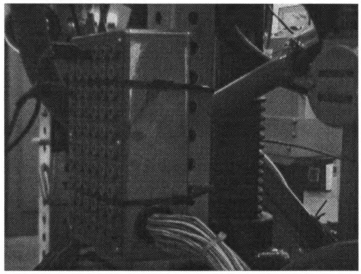

Fig. C.17: Ford Controller Breakout Box

Table C.4: EEC Breakout Box Pinout Chart

Pin #	Circuit	Circuit Function	Pin #	Circuit	Circuit function
1	330 (DB/R)	Keep Alive Power	31	386 (R/BK)	Cooling Fan Hi speed output (n/a)
2	-	NOT USED	32	-	NOT USED
3	150 (W/BK)	Vehicle Speed Sensor (VSS) DIF (+) (n/a)	33	108 (W/DB)	EGR Vacuum Regulator (EVR) (n/a)
4	153 ®	Identification Diagnostic Monitor (IDM)	34	63 (LG/BK)	Signal return (NOT USED)
5	-	NOT USED	35	719 (Y/W)	Cooling Fan Lo speed output (n/a)
6	57 (DB)	Vehicle Speed Sensor (VSS) DIF (-) (n/a)	36	156 (LG/W)	Spark Angle Word (SAW)
7	62 (DB/W)	Engine Coolant Temperature (ECT)	37	101 (W/R)	V PWR (?)
8	121 (Y/DG)	Data (-) (?)	38	-	NOT USED
9	87 (DG/Y)	Mass Air flow return	39	-	NOT USED
10	707 (DG/BK)	A/C On Input (n/a)	40	599 (BK/DG)	Ground
11	-	NOT USED	41	128 (O)	CID (?)
12	105 (Y/O)	Injector #3 Output	42	127 (DB/DG)	CID (?)
13	115 (DG/O)	Injector #4 Output	43	171 (DG/W)	Octane Adjust (?)
14	-	NOT USED	44	-	NOT USED
15	94 (O/W)	Canister Purge Solenoid Output (n/a)	45	-	NOT USED
16	78 (R/DB)	Ignition Ground	46	63 (LG/BK)	Signal return
17	129 (Y/BK)	STO/MIL = EEC Control line	47	71 (R/W)	Throttle Position
18	-	NOT USED	48	118 (LG/Y)	STI = EEC Control Line
19	102 (BK/PK)	Fuel Pump Relay Output (FPM) (n/a)	49	85 (O/BK)	HEGO ground
20	-	NOT USED	50	143 (BR/BK)	Mass Air Flow
21	83 (DB/O)	Idle Speed Control Valve (ISC)	51	-	NOT USED
22	103 (LG)	Fuel Pump Relay Input (FP)	52	-	NOT USED
23	-	NOT USED	53	154 (LG/R)	Shif indicator light (n/a)
24	-	NOT USED	54	702 (DB/BK)	WOT (A/C cutout (W/C)) (n/a)
25	109 (W/DG)	Air Charge Temperature (ACT)	55	-	NOT USED
26	85 (LG/W)	VREF	56	69 (DG/W)	Profile Ignition Pickup (PIP)
27	145 (DB/Y)	PFE	57	101 (W/R)	V PWR (?)
28	122 (Y/DB)	Data (+) (?)	58	106 (Y)	Injector #1 Output
29	116 (DG/DB)	HEGO Input	59	116 (DG/R)	Injector #2 Output
30	62 (BR/Y)	Park/Neutral Input or Clutch Interrupt Sw. Input (n/a)	60	999 (BK/DG)	Ground

C.5.2 Control Signal Monitoring

The most important I/O signals are given below. Remark that some sensor signals have a separate ground shielded from the ignition ground.

Injector #1 output: between pin 58 & ground

Injector #2 output: between pin 59 & ground

Injector #3 output: between pin 12 & ground

Injector #4 output: between pin 13 & ground

Spark: between pin 16 & ground OR from inductive pickup probe around spark wire

Mass airflow: between pin 50 & pin 9

HEGO Sensor: between pin 29 and pin 49

IAC valve input: between pin 21 and ground

C.5.3 Measuring Spark Advance

To monitor spark signals on the oscilloscope, use the signal from the Hall effect sensor on the camshaft (occurs once every engine cycle) as a trigger. The cam signal is obtained from the Cosworth front panel BNC connector labeled "sync". Make sure the triggering is stable before proceeding. Every trigger event, spark plugs fire twice (dual coil system): cylinders #1 and #4 fire together and cylinders #3 and #2 fire together. The firing sequence is 1-3-4-2.

The Hall effect trigger signal was calibrated to occur at 41.6 degrees BTDC compression of the first cylinder in the firing sequence (cylinder #1). The time interval Δt_{SA} between the occurrence of the trigger and the occurrence of the spark is related to spark advance SA [deg BTDC] through *RPM* and the number n_i of the plug *i* in firing sequence:

$$SA = -41.6° + \frac{RPM}{60} \cdot \Delta t_{SA} \cdot 360° - (n_i - 1) \cdot 180° \qquad \text{(C.1)}$$

TO OBTAIN A CLEAR SPARK SIGNAL USING AN INDUCTIVE PROBE AROUND THE SPARK WIRE, MAKE SURE THAT:

1. the probe doesn't touch other spark wires
2. the probe doesn't touch the engine block
3. the probe is put around the wire near the coil (NOT near the spark plug)

For #1 and #2: the probe may pick up interference from other spark plugs. For #3: it has been observed that when the probe touches the spark wire near the spark plug, the trigger (cam signal) may disappear and the oscilloscope display for the spark becomes unsteady. This is due to formation of small static charges on the outside of the spark wires near the spark plug. These charges raise the voltage potential of the probe ground above engine (AND oscilloscope) ground, from which results a ground loop through the oscilloscope to the Hall effect sensor.

C.5.4 Measuring Injection Timing

Use the signal from the Hall effect sensor on the camshaft (occurs once every engine cycle) as a trigger. The injector phase angle (= the crank angle at which injection starts) can be measured the same way as spark advance (equation C.1). The fuel injector pulse width is the time the injector signal stays low.

C.6 Control System Operation and Mapping

The EEC outputs signals to the EDIS for firing the spark, actuates the IAC valve and fires the fuel injectors based on the input signals it receives from the sensors. No detailed information was available on the code currently loaded into

the EEC micro-controller. Through elaborate testing of the engine in different regimes, engine maps were extracted. The maps currently downloaded into the EEC were found not to be compatible with engine mapping information received from Ford (Appendix D). This section gives as much information on the current EEC settings as could be obtained through dynamometer tests.

C.6.1 Base Spark and Fuel Maps in terms of Throttle Angle

To generate base spark and base fuel injection timing maps, it was assumed that the EEC uses the signal from the throttle position sensor as a measure of engine load. This instead of using the signal from the MAF sensor, which tends to be reliable only in a specific load-speed region. Base spark timing consists of a map of spark advance *SA* as a function of engine *RPM* and throttle angle θ (Table C.5, Fig. C.18). Base injection timing consists of a map of injector flow rate $\dot{m}_f$ as a function of engine *RPM* and throttle angle θ (Table C.6, Fig. C.19).

The base fuel injection map uses flow rate $\dot{m}_f$ instead of injector pulse width *PW* as the mapped variable. This has the advantage that the map becomes independent of the type of injectors used. For convenience, a fuel map for the *PW* of the injectors on the engine (FOSE-9F593-A1A, *offset* = 0.8 ms, injector flow rate $\dot{m}_{f0}$ = 6.44 kg/hr) is given in Table C.7. The pulse width given is the OVERALL pulse width, i.e. including injector offset. For conversion of *PW* into fuel flow rate $\dot{m}_f$, use:

$$\dot{m}_f = \dot{m}_{f0} \cdot \frac{PW - offset}{1000} \cdot \frac{RPM}{120} \cdot n \qquad \text{(C.2)}$$

with n = number of cylinders, *PW* and *offset* in [ms]

An inductive probe for the spark on cylinder #1 generated the spark signal. The signal from injector #1 was obtained from the breakout box. How to calculate spark advance and injector pulse from an oscilloscope measurement is discussed in section C.5.

The HEGO feedback control (see later in this section) slightly alters the fuel injector *PW* over time. Pulse width measurements were made with the HEGO feedback mode activated. To somehow compensate for these changes in fuel injector pulse width, two measurements were made and the average calculated. Base fuel flow rates and base pulse widths shown in Table C.6 and Table C.7 correspond to the average values.

C.6.2 Discussion of the Base Timing

The base spark timing map is surprisingly not very dependent on the speed–load operating conditions. Spark advance varies from 10 to 14 degrees only, whereas one would expect values of up to 20 or even 30 degrees advance at high *RPM*. Spark advance is set very conservative, at a value much lower than *MBT* (minimum advance for best torque). The engine can clearly output more power than is obtained with the spark settings downloaded in the EEC.

The fuel table shows that at high *RPM* and load, the injectors are near their full capacity of 4*6.44 = 25.8 kg/hr. The injectors almost continuously spray fuel at those conditions.

Table C.5: Spark Advance = $f(RPM, \theta)$

SA [°]	*θ* [°]							
RPM	10	20	30	40	50	60	70	80
1200	10.9	10.6						
1400	11.7	11.9	12.2	12.6				
1600	11.9	12.1	12.7	12.5	12.6	12.6	12.4	12.4
1800	12.2	12.6	12.8	12.3	12.6	12.9	12.9	12.9
2000	12.5	12.3	12.8	12.8	12.7	12.9	12.7	12.7
2200	12.4	12.5	12.7	12.4	13.1	13.1	13.1	13.1
2400		12.5	12.8	12.8	12.9	12.9	13.4	13.4
2600		12.5	13.1	13.1	13.6	13.3	13.6	13.6
2800		12.5	12.2	12.2	12.7	12.5	12.7	12.7
3000		13.6	13.9	14.3	14.1	14.5	14.8	14.8
3200		13.9	13.5	13.1	13.7	13.9	13.7	13.7
3400		13.9	13.3	13.7	13.5	14.3	13.9	13.9
3600		14.2	13.7	13.7	14.4	14.0	14.0	14.0
3800		13.9	13.5	13.0	13.3	13.7	13.7	13.7
4000		14.3	14.6	14.3	14.1	13.6	13.6	13.6
4200			12.9	13.2	13.2	13.2	13.4	13.4

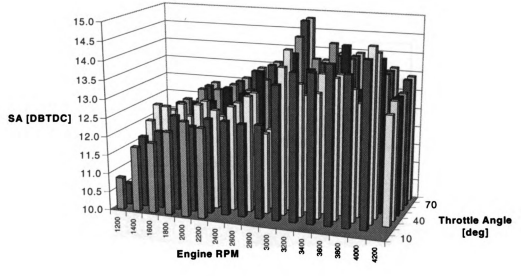

Fig. C.18: Base Spark Advance Map

Table C.6: Fuel Flow Rate = $f(RPM, \theta)$

$\dot{m}_f$ [kg/hr]	θ [°]							
RPM	10	20	30	40	50	60	70	80
1200	3.61	3.84						
1400	4.06	4.61	4.78	4.72				
1600	4.26	5.05	5.15	5.48	5.60	5.70	5.87	7.42
1800	4.52	5.58	5.93	6.20	6.32	6.66	6.66	6.43
2000	4.94	6.12	6.70	6.93	6.85	7.49	7.53	7.23
2200	4.98	6.61	7.51	7.67	7.89	8.10	8.48	8.57
2400		7.03	8.60	8.58	8.99	9.09	9.38	9.30
2600		7.20	9.24	9.49	9.57	9.79	9.93	10.18
2800		8.23	10.10	10.55	10.64	11.03	11.09	11.12
3000		9.01	11.62	11.94	12.01	12.30	12.30	12.43
3200		9.82	12.67	13.53	13.63	14.01	13.87	14.25
3400		10.40	13.32	14.60	15.00	15.32	15.18	15.43
3600		10.78	14.37	15.88	16.30	16.42	16.50	16.65
3800		11.01	15.09	17.09	17.58	17.82	17.98	18.15
4000		11.33	15.63	17.94	18.33	18.80	19.36	19.57
4200			16.14	18.57	19.43	20.06	20.19	20.33

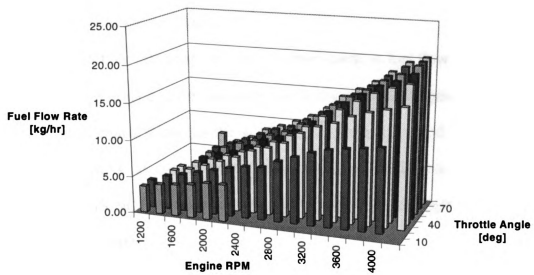

Fig. C.19: Base Fuel Flow Rate Map

Table C.7: Injector $PW = f(RPM, \theta)$ [FOSE-9F593-A1A only]

$\dot{m}_f$ [kg/hr]	θ [°]							
RPM	10	20	30	40	50	60	70	80
1200	14.80	15.70						
1400	14.30	16.15	16.70	16.50				
1600	13.20	15.50	15.80	16.75	17.10	17.40	17.90	22.40
1800	12.50	15.25	16.15	16.85	17.15	18.05	18.05	17.45
2000	12.30	15.05	16.40	16.95	16.75	18.25	18.35	17.65
2200	11.35	14.80	16.70	17.05	17.50	17.95	18.75	18.95
2400		14.45	17.50	17.45	18.25	18.45	19.00	18.85
2600		13.70	17.35	17.80	17.95	18.35	18.60	19.05
2800		14.50	17.60	18.35	18.50	19.15	19.25	19.30
3000		14.80	18.85	19.35	19.45	19.90	19.90	20.10
3200		15.10	19.25	20.50	20.65	21.20	21.00	21.55
3400		15.05	19.05	20.80	21.35	21.80	21.60	21.95
3600		14.75	19.40	21.35	21.90	22.05	22.15	22.35
3800		14.30	19.30	21.75	22.35	22.65	22.85	23.05
4000		14.00	19.00	21.70	22.15	22.70	23.35	23.60
4200			18.70	21.40	22.35	23.05	23.20	23.35

C.6.3 Map Boundaries and Blanks

The base fuel flow rate map shows a sudden peak in fuel flow at low *RPM* and high load. The engine is not meant to run in this regime: logging occurs. For the same reason, maps show blanks at higher throttle angles and low *RPM*. Maps also show blanks at low throttle angles and high *RPM*: this is the region of backfiring. IT IS NOT ADVISABLE TO RUN THE ENGINE OUTSIDE THE *RPM* REGIONS SHOWN.

Maps stop at 80 degrees throttle: no significant differences were seen between the settings at 80 degrees throttle and those at WOT. Maps stop at 1200 *RPM* because the setup has a resonance at about 1000 *RPM*. The dynamometer is

not meant to run below 800 RPM. Maps stop at 4200 *RPM* because of dynamometer *RPM* and safety limitations.

C.6.4 Base Spark and Fuel Maps in terms of Manifold Pressure and Cylinder Air Charge

The air intake variable directly associated with the combustion process is the cylinder air charge m_{ac}. The engine load is strictly proportional to the air charge. The aim of the control system is to set spark and fuel injection timing for a given air charge and engine *RPM*. Spark advance is used to set the engine torque (or mechanical power). Fuel injection sets the air to fuel ratio. The air to fuel ratio influences emissions in the exhaust as well as specific fuel consumption.

The base timing maps given in Table C.5 and Table C.6 use throttle angle as a measure of engine load, assuming the cylinder air charge depends on throttle angle and *RPM* only. This approach is not entirely correct due to the action of the idle air control valve. The intake airflow is a function of engine *RPM*, throttle angle AND idle air control valve duty cycle. This means that for a given throttle angle and *RPM*, the cylinder air charge may still vary for different IAC valve duty cycles. It is therefor more appropriate to use the mean manifold pressure p_m or the cylinder air charge m_{ac} as a mapping variable for engine load.

Manifold pressure is the preferred variable since it can much more accurately be measured than the cylinder air charge (or mass airflow in the intake). For the running conditions of Table C.5 and Table C.6 (i.e. with the IAC valve actuated by the EEC), Table C.8 and Table C.9 give manifold pressure and mass airflow as a function of throttle angle and engine *RPM*. Elimination of the throttle angle

out of a combination of Table C.8 and Table C.9 with Table C.5 and Table C.6 yields maps for spark and fuel injection timing as a function of air charge or manifold pressure. These maps were not generated due to time constraints.

Airflow and manifold pressure vary with environmental conditions (pressure p_0 and temperature T_0). THE MAPS REPRESENTED WERE TAKEN AT:

$$p_0 = 96.3 \text{ kPa} \qquad (C.3)$$
$$T_0 = 297.6 \text{ K}$$

Dependency of the maps on environmental conditions can be avoided by expressing them in terms of dimensionless variables. If one assumes that the **manifold temperature T_m is approximately equal to the environmental temperature T_0**, a set of dimensionless variables is given by:

$$\begin{aligned}
&\frac{\theta}{\theta_{ref}} \text{ with } \theta_{ref} = 90° \\
&\frac{p_m}{p_{ref}} \text{ with } p_{ref} = p_0 \\
&\frac{\dot{m}_a}{\dot{m}_{ref}} \text{ with } \dot{m}_{ref} = 0.685 \cdot \frac{p_0}{\sqrt{r \cdot T_0}} \cdot A_i \\
&\frac{RPM}{RPM_{ref}} \text{ with } RPM_{ref} = \frac{\sqrt{r \cdot T_0}}{V_c} \cdot A_i
\end{aligned} \qquad (C.4)$$

The constant r equals 287 J/(kg K). $\dot{m}_{ref}$ is the airflow for choked flow through the intake (minimum area A_i) at wide-open throttle. For the current intake system on the engine, A_i could be chosen equal to 1.338 E-3 m^2 (inner diameter of the MAF sensor = 1 5/8"). V_c is the displaced volume of the cylinder and equals 0.4646 E-3. For ease of comparison with the axes of the spark and fuel injection timing maps (Table C.5 and Table C.6) as well as to get a feeling for the absolute values of manifold pressure and mass airflow in the intake, maps were not

presented in dimensionless form. WHENEVER USING THE MAPS OF TABLE C.8 AND TABLE C.9, TAKE INTO ACCOUNT THE CHANGE OF THE MAPPED VARIABLES AND THE MAP AXES WITH THE ENVIRONMENTAL CONDITIONS (c.3) THROUGH EQUATIONS C.4.

A map for air charge can be derived from the mass airflow map through multiplication with the period of an intake stroke:

$$m_{ac} = \dot{m}_a \cdot \frac{120}{RPM} \tag{C.5}$$

Mapped airflow and manifold pressure represent mean values only. Real airflow and pressure are fluctuating due to the intake pulses. Mean values were obtained in the following way. For manifold pressure, the mean voltage output of a manifold pressure sensor was calculated using the voltage averager of the digital oscilloscope. Mean voltage was then related to manifold pressure through sensor calibration.

For mass airflow, the situation is much more complicated: mass airflow is very hard to measure directly. To measure mass airflow, fuel injector pulse width was adjusted until the HEGO sensor in the exhaust system showed stoichiometric combustion. Stoechiometry was defined as the operating condition for which the HEGO sensor switches between rich and lean voltage levels AND thereby stays rich as long as it stays lean. The injector pulse width at stoechiometry was recorded as a function of throttle angle and *RPM.* Fuel flow was calculated using (C.2). At stoechiometry, the mass airflow rate in the intake is approximately 14.6 times the fuel flow rate. Due to the nonlinear HEGO sensor voltage

characteristics as a function of air to fuel ratio, the measure for stoechiometry might be off by a constant factor.

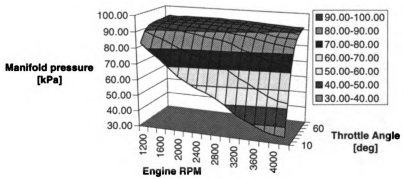

Fig. C.20: Manifold Pressure @ p_0 = 96.3 kPa, T_0 = 24.5 °C

C.6.5 Cold Start Enrichment

During engine warm-up the base fuel flow rate of Table C.6 is multiplied by a constant that depends on the elapsed time after startup was initiated, on the engine coolant (or block temperature) or on both. Cold start enrichment was not studied in detail. For a single test run at 1400 rpm and 10 % throttle, it was observed that cold start enrichment was applied up to a block temperature of about 140 °F, which was reached 3 minutes after startup. For the test run, Table C.10 gives values for the cold start enrichment multiplier as a function of block temperature.

Table C.8: Manifold Pressure $p_m = f(RPM, \theta)$

p_m [kPa]	θ [°]							
RPM	10	20	30	40	50	60	70	80
1200	83.35	89.76	92.28	93.07	93.45	93.45	93.84	93.84
1400	78.30	87.24	91.90	92.87	93.07	93.45	93.45	93.45
1600	74.41	85.29	91.12	92.68	93.07	93.45	93.45	93.84
1800	69.36	82.57	90.54	92.28	93.07	93.45	93.84	93.84
2000	64.32	79.86	89.57	91.90	93.07	93.45	93.84	93.84
2200	61.21	77.91	88.79	91.51	92.68	93.45	93.84	93.84
2400	58.10	76.36	87.62	91.12	92.68	93.45	93.64	93.84
2600	56.15	74.81	86.85	90.74	92.28	93.07	93.45	93.45
2800	53.25	72.48	86.07	89.95	91.51	93.07	93.07	93.45
3000	49.55	69.36	84.32	89.18	91.12	92.68	92.68	93.07
3200	44.78	65.49	81.41	88.41	90.74	92.28	92.68	92.68
3400	41.86	62.76	79.86	87.24	89.95	91.71	92.28	92.28
3600	39.07	59.27	77.53	86.07	89.18	90.74	91.51	91.90
3800	36.54	56.15	75.58	84.90	88.01	89.95	91.12	91.51
4000	35.06	53.82	74.03	84.13	87.62	89.95	90.74	91.12
4200	34.67	53.05	72.67	83.16	87.24	89.18	90.34	91.12

Table C.9: Mass Airflow $\dot{m}_a = f(RPM, \theta)$

$\dot{m}_a$ [kg/hr]	θ [°]							
RPM	10	20	30	40	50	60	70	80
1200	50.69	55.96						
1400	56.40	65.50	67.46	68.59				
1600	60.72	73.62	76.05	78.42	80.03	80.94	81.91	81.72
1800	64.78	81.29	85.73	88.44	89.87	90.82	91.69	91.01
2000	68.48	88.68	96.55	99.96	101.22	102.56	103.29	103.03
2200	70.59	94.84	106.36	109.68	111.00	112.52	113.59	113.03
2400		100.80	115.17	118.93	120.38	122.11	122.98	122.59
2600		104.51	120.50	125.99	127.14	129.26	130.07	130.19
2800		109.41	127.73	134.59	135.62	138.12	139.16	138.97
3000		113.55	135.84	144.84	145.32	149.02	149.65	149.91
3200		118.08	147.34	159.33	162.59	165.24	166.16	166.69
3400		120.63	154.07	170.07	173.85	176.93	178.13	178.21
3600		123.52	162.62	181.21	186.43	190.15	193.07	192.58
3800		125.53	171.68	193.40	200.95	206.09	206.59	208.89
4000		127.60	177.11	202.37	210.76	216.52	218.64	219.87
4200			180.31	210.32	219.45	225.72	228.47	229.47

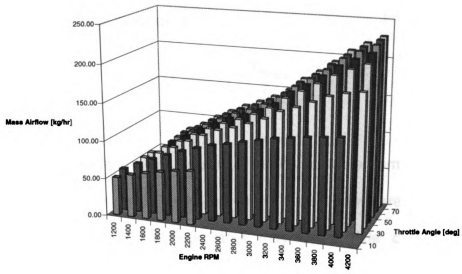

Fig. C.21: Mass Airflow @ p_0 = 96.3 kPa, T_0 = 24.5 °C

Table C.10: Cold Start Multiplier as a Function of Block Temperature (1400 rpm, 10% throttle)

T_{block} [°F]	85	89	96	100	108	114	125	132	140
$multiplier_{ECT}$	1.38	1.34	1.28	1.20	1.17	1.11	1.07	1.02	1.00

C.6.6 Air Charge Temperature Trimming of Fuel Injection

Fuel injection maps are set to have the engine run at particular air to fuel ratio conditions dependent on engine *RPM* and engine load. The mapping entries are however dependent on the environmental conditions. Changes in environmental conditions will then cause changes in air to fuel ratio. A change in temperature is accounted for by means of the air charge temperature multiplier. Since manifold density varies inversely proportional to manifold (or intake) temperature, the same will be true for the mass airflow into the cylinder. Base fuel flow rates are then multiplied with a constant based on a measurement of the actual manifold

temperature T_m, with respect to the reference manifold temperature T_{mMAP} for which the fuel map was calculated:

$$multiplier_{ACT} = \frac{T_{mMAP}}{T_m} \tag{C.6}$$

C.6.7 HEGO Trimming of Fuel Injection

At low *RPM* and throttle angles, passenger car engines are normally tuned to run at low emissions and high mileage. Air to fuel ratios are then set near stoechiometry. Base injector flow rates may be a little off stoichiometric conditions. Also, environmental operating conditions may change, altering the air to fuel ratio. To compensate for these errors, at low RPM and throttle angle, the engine controller runs in HEGO feedback mode. In this control mode a signal from the HEGO sensor is fed back into the controller. The signal indicates whether the engine runs rich or lean. If the engine runs rich, the fuel pulse width is decreased until the HEGO indicates lean condition. From that moment on, the pulse width is increased again until the engine runs rich, and so on. The HEGO sensor continuously switches between rich and lean conditions as fuel pulse widths ramp up and down. The specific algorithm for the HEGO feedback could not be obtained from Ford. The following information could however be extracted through oscilloscope measurements:

1. The HEGO feedback has about 0.3 milliseconds worth of authority to change the injector pulse width
2. The HEGO feedback is only active in certain throttle-*RPM* regions (low throttle and low *RPM*). At high *RPM* and throttle, the engine runs rich and

HEGO is not active. This means that in these regions it was tuned to generate power instead of running efficiently.

Table C.11 gives measurements for the relative air to fuel ratio λ as a function of *RPM* and throttle angle. The shaded regions indicate the load-speed domain in which the HEGO feedback was found to be activated (HEGO sensor voltage switching). Outside the shaded region, the HEGO sensor was not active. As can be observed from the table, this region primarily corresponds to rich conditions ($\lambda < 0.95$). High values for lambda outside the shaded region are due to the base pulse width setting being close to stoechiometry: the HEGO feedback needs not to be active to yield stoichiometric combustion.

Table C.11: Relative A/F Ratio $\lambda = (A/F)/(A/F)_{stoech}$ as related to HEGO Feedback

λ	θ [°]							
RPM	10	20	30	40	50	60	70	80
1200	0.96	1.00						
1400	0.95	0.97	0.97	1.00				
1600	0.98	1.00	1.01	0.98	0.98	0.97	0.96	0.75
1800	0.98	1.00	0.99	0.98	0.97	0.93	0.94	0.97
2000	0.95	0.99	0.99	0.99	1.01	0.94	0.94	0.98
2200	0.97	0.98	0.97	0.98	0.96	0.95	0.92	0.90
2400		0.98	0.92	0.95	0.92	0.92	0.90	0.90
2600		0.99	0.89	0.91	0.91	0.90	0.90	0.88
2800		0.91	0.87	0.87	0.87	0.86	0.86	0.86
3000		0.86	0.80	0.83	0.83	0.83	0.83	0.83
3200		0.82	0.80	0.81	0.82	0.81	0.82	0.80
3400		0.79	0.79	0.80	0.79	0.79	0.80	0.79
3600		0.78	0.78	0.78	0.78	0.79	0.80	0.79
3800		0.78	0.78	0.78	0.78	0.79	0.79	0.79
4000		0.77	0.78	0.77	0.79	0.79	0.77	0.77
4200			0.77	0.78	0.77	0.77	0.77	0.77

C.7 Engine Startup and Shutdown Procedures

C.7.1 Engine Startup (using the Ford EEC)

1. Follow the safety check instructions of Appendix B.1
2. Follow the pre-run check and running preparation instructions of Appendix B.2
3. Follow the dynamometer startup instructions of Appendix B.3 till step # 14.
4. Pull out the emergency switch (yellow box mounted at the bottom of the dynamometer control panel) and turn on the fuel pump (manual operator panel switch up) to allow the fuel to pressurize and air bubbles to escape from the fuel lines. Fuel pressure on the gauge should show about 35-40 psi with the engine not running. The engine will have a rough start if this step is skipped.
5. Push the emergency switch to disconnect power from the operator panel and turn on the ignition switch and the fuel pump switch on the operator panel (both manual switches up).
6. Proceed with steps 15 and 16 of appendix B.5 to bring the engine at high idle (1200 *RPM*)
7. To fire the engine, pull out the emergency switch.
8. Allow engine warm-up before continuing. For smooth warm-up, run the engine at about 10 % throttle and 1400 rpm. It will take approximately 3 minutes for the engine block to reach 140 °F and about 6 minutes to get up to steady temperature (190-195°F). The engine is warm if the thermostat opens:

the hose connecting the thermostat housing to the coolant valves will then be hot.

C.7.2 Engine Shutdown

1. Gradually remove the load on the engine (either throttle position or torque).
2. Allow the engine to "idle" by turning down the "Speed" knob until 1200 *RPM* (engine setup has a resonance at about 1000-1100 *RPM*).
3. Idle the engine for about 5-10 minutes to allow the oil to cool down to approximately 200º F.
4. Push the emergency stop button (yellow box mounted at the bottom of the dynamometer control panel) to turn off the ignition and the fuel pump.
5. Follow the instructions of Appendix B.5 for dynamometer shutdown.

C.8 Remaining Tasks

As for facility development, the following tasks remain. The exhaust pipe needs to be cut to size and welded together. Additional exhaust heat shields need to be put up in order to avoid melting of the coolant hose leaving the engine. The coolant hose entering the engine needs to be extended in order to keep it away from the muffler. The rotor of the exhaust fan needs to be welded onto its shaft to avoid loosening at high exhaust temperatures.

The Cosworth IC5460 Engine Control System ® has only been run in its manual control mode. In order to run the system in its more advanced table control modes, the base timing maps received from Ford need to be converted into the form required by the IC5460. It is advisable to use the manifold pressure as a

measure for engine load instead of throttle angle or mass airflow. The internal IC5460 system chip is currently set up to run off the manifold pressure sensor. In order to run the Cosworth system in table control mode, an emergency switch needs to be installed, since ignition and fuel injection cannot be shut off from the host program. The 12-volt line connecting battery power to the distributorless ignition box needs to be run through the emergency switch. The red jumper wire (which connects the internal voltage supply to the fuel injector power input) at the back panel of the Cosworth System will have to be run through the emergency switch as well.

APPENDIX D

MAIN DOCUMENT DATA SHEETS

This appendix lists the data used in the main document.

Table D.1: Friction Torque = $f(RPM,\theta)$, refer to Fig. 6

T_f [Nm]	θ [°]							
RPM	10	20	30	40	50	60	70	80
1200	12.2	11.8						
1400	12.9	12.2	12.2	12.3				
1600	13.7	12.8	12.7	13	12.6	12.6	12.6	12.8
1800	14.8	13.7	13.6	13.7	13.3	13.3	13.3	13.4
2000	16	14.8	14.5	14.8	14.1	14.1	14.1	14.3
2200	17.2	16.2	15.6	15.6	15	15	15	15.4
2400		17.1	16.4	16.3	16	16	16	16.2
2600		17.8	17.2	17.1	16.4	16.4	16.4	16.6
2800		18.5	17.8	17.7	17.4	17.4	17.4	17.7
3000		19.5	18.9	18.9	18.3	18.3	18.3	18.4
3200		20.7	19.8	19.9	19.2	19.2	19.2	19.5
3400		21.3	21	20.8	20.3	20.3	20.3	20.5
3600		22.5	21.9	22.1	21.8	21.8	21.8	21.7
3800		23.5	23	23.2	22.7	22.7	22.7	22.7
4000		23.8	23.5	23.9	23.3	23.3	23.3	23.9
4200			25	24.8	24.5	24.5	24.5	24.5

Table D.2: Gross Indicated Torque = $f(RPM,\theta)$, refer to Fig. 7 (@ 97.1 kPa, 24.5 °C)

T_i [Nm]	θ [°]							
RPM	10	20	30	40	50	60	70	80
1200	87.3	96.2						
1400	86.5	99.4	101.3	102.5				
1600	81.8	97.9	101.7	104	104.9	109.3	109.1	109.5
1800	77.3	96.4	102.6	105.3	106.3	109.9	109.5	109.8
2000	73.3	94.4	103.7	107.1	107.6	110.9	110.5	111
2200	67.1	91	104.7	106.1	106.4	112.5	112.2	112.4
2400		88.2	104.3	107.4	108.8	112.3	112.1	111.3
2600		86.4	102.5	105.8	107.4	110.9	110.7	110.2
2800		86.5	101.8	105.9	107.4	110.6	110.8	110.4
3000		84.8	101	106.5	108.1	111.9	111.8	111
3200		83.5	102	109.7	111.4	115.5	115.8	115.8
3400		79.8	102	110.4	112.9	116.8	117.6	117.4
3600		77.3	100.5	111.7	114.8	119.5	120	119.6
3800		74.6	100.2	112.8	116.1	121.3	122.1	121.9
4000		70.3	97.3	110.9	114.5	119.5	120.8	121.4
4200			93.3	108.4	112.9	118.5	119.7	119.9

Table D.3: Mechanical Efficiency = $f(RPM,\theta)$, refer to Fig. 8

η_m	θ [°]							
RPM	10	20	30	40	50	60	70	80
1200	0.86	0.88						
1400	0.85	0.88	0.88	0.88				
1600	0.83	0.87	0.88	0.88	0.88	0.88	0.88	0.88
1800	0.81	0.86	0.87	0.87	0.87	0.88	0.88	0.88
2000	0.78	0.84	0.86	0.86	0.87	0.87	0.87	0.87
2200	0.74	0.82	0.85	0.85	0.86	0.87	0.87	0.86
2400		0.81	0.84	0.85	0.85	0.86	0.86	0.85
2600		0.79	0.83	0.84	0.85	0.85	0.85	0.85
2800		0.79	0.83	0.83	0.84	0.84	0.84	0.84
3000		0.77	0.81	0.82	0.83	0.84	0.84	0.83
3200		0.75	0.81	0.82	0.83	0.83	0.83	0.83
3400		0.73	0.79	0.81	0.82	0.83	0.83	0.83
3600		0.71	0.78	0.80	0.81	0.82	0.82	0.82
3800		0.68	0.77	0.79	0.80	0.81	0.81	0.81
4000		0.66	0.76	0.78	0.80	0.81	0.81	0.80
4200			0.73	0.77	0.78	0.79	0.80	0.80

Table D.4: SAI Multiplier, refer to Fig.9 (SA-MBT in ° crank)

SA-MBT	SAI	SA-MBT	SAI
-25.5	0.695	-10.5	0.949
-24.5	0.720	-9.5	0.958
-23.5	0.740	-8.5	0.966
-22.5	0.764	-7.5	0.974
-21.5	0.786	-6.5	0.980
-20.5	0.800	-5.5	0.986
-19.5	0.820	-4.5	0.990
-18.5	0.843	-3.5	0.989
-17.5	0.859	-2.5	0.995
-16.5	0.875	-1.5	0.997
-15.5	0.891	-0.5	1.000
-14.5	0.901	0.5	1.000
-13.5	0.916	1.5	1.000
-12.5	0.926	2.5	0.998
-11.5	0.939	3.5	0.997

Table D.5: AFI Multiplier, refer to Fig.10

λ	AFI	λ	AFI	λ	AFI	λ	AFI	λ	AFI
0.685	0.675	0.763	0.773	0.861	0.889	0.987	0.997	1.156	0.989
0.69	0.68	0.768	0.779	0.867	0.897	0.995	0.998	1.168	0.991
0.694	0.686	0.773	0.786	0.874	0.904	1.004	1.001	1.180	0.986
0.698	0.691	0.779	0.792	0.881	0.911	1.013	1.003	1.192	0.978
0.702	0.696	0.784	0.799	0.887	0.917	1.022	1.009	1.205	0.948
0.707	0.702	0.789	0.806	0.894	0.924	1.031	1.005	1.218	0.947
0.711	0.707	0.795	0.813	0.901	0.93	1.041	1.008	1.231	0.952
0.715	0.713	0.801	0.819	0.909	0.937	1.05	1.01	1.244	0.934
0.72	0.719	0.806	0.826	0.916	0.944	1.06	1.008	1.258	0.911
0.725	0.724	0.812	0.832	0.923	0.952	1.07	1.011	1.272	0.906
0.729	0.73	0.818	0.838	0.931	0.959	1.08	1.009	1.286	0.865
0.734	0.735	0.824	0.845	0.938	0.965	1.09	1.005	1.301	0.855
0.739	0.742	0.83	0.851	0.946	0.972	1.101	1.006	1.316	0.823
0.743	0.749	0.836	0.859	0.954	0.976	1.111	1.004		
0.748	0.755	0.842	0.866	0.962	0.983	1.122	1		
0.753	0.761	0.848	0.873	0.97	0.985	1.133	0.998		
0.758	0.767	0.854	0.88	0.978	0.99	1.145	0.994		

Table D.6: In-Cylinder Fuel Mass, refer to Fig.13

m_{fc} [kg]	θ [°]							
RPM	10	20	30	40	50	60	70	80
1200	2.504E-05	2.665E-05						
1400	2.415E-05	2.746E-05	2.844E-05	2.809E-05				
1600	2.218E-05	2.630E-05	2.683E-05	2.853E-05	2.916E-05	2.970E-05	3.059E-05	
1800	2.093E-05	2.585E-05	2.746E-05	2.871E-05	2.925E-05	3.086E-05	3.086E-05	2.979E-05
2000	2.057E-05	2.549E-05	2.791E-05	2.889E-05	2.853E-05	3.122E-05	3.140E-05	3.014E-05
2200	1.887E-05	2.504E-05	2.844E-05	2.907E-05	2.987E-05	3.068E-05	3.211E-05	3.247E-05
2400		2.442E-05	2.987E-05	2.979E-05	3.122E-05	3.157E-05	3.256E-05	3.229E-05
2600		2.308E-05	2.961E-05	3.041E-05	3.068E-05	3.140E-05	3.184E-05	3.265E-05
2800		2.451E-05	3.005E-05	3.140E-05	3.166E-05	3.283E-05	3.301E-05	3.309E-05
3000		2.504E-05	3.229E-05	3.318E-05	3.336E-05	3.417E-05	3.417E-05	3.453E-05
3200		2.558E-05	3.301E-05	3.524E-05	3.551E-05	3.649E-05	3.614E-05	3.712E-05
3400		2.549E-05	3.265E-05	3.578E-05	3.676E-05	3.757E-05	3.721E-05	3.784E-05
3600		2.496E-05	3.327E-05	3.676E-05	3.775E-05	3.801E-05	3.819E-05	3.855E-05
3800		2.415E-05	3.309E-05	3.748E-05	3.855E-05	3.909E-05	3.945E-05	3.980E-05
4000		2.361E-05	3.256E-05	3.739E-05	3.819E-05	3.918E-05	4.034E-05	4.079E-05
4200			3.202E-05	3.685E-05	3.855E-05	3.980E-05	4.007E-05	4.034E-05

Table D.7: Indicated Fuel Conversion Efficiency = $f(RPM,\theta)$, refer to Fig. 14

η_f	θ [°]							
RPM	10	20	30	40	50	60	70	80
1200	0.337	0.350						
1400	0.347	0.351	0.345	0.353				
1600	0.357	0.360	0.367	0.353	0.349	0.356	0.345	
1800	0.358	0.361	0.362	0.355	0.352	0.345	0.343	0.357
2000	0.345	0.358	0.360	0.359	0.365	0.344	0.341	0.357
2200	0.344	0.352	0.357	0.353	0.345	0.355	0.338	0.335
2400		0.350	0.338	0.349	0.337	0.344	0.333	0.334
2600		0.363	0.335	0.337	0.339	0.342	0.337	0.327
2800		0.342	0.328	0.327	0.329	0.326	0.325	0.323
3000		0.328	0.303	0.311	0.313	0.317	0.317	0.311
3200		0.316	0.299	0.301	0.304	0.307	0.310	0.302
3400		0.303	0.302	0.299	0.297	0.301	0.306	0.300
3600		0.300	0.292	0.294	0.295	0.304	0.304	0.300
3800		0.299	0.293	0.291	0.292	0.301	0.300	0.297
4000		0.288	0.289	0.287	0.290	0.295	0.290	0.288
4200			0.282	0.285	0.284	0.288	0.289	0.288

Table D.8: In-Cylinder Fuel Mass at Stoechiometry, refer to Fig.15

m_{fc} [kg]	θ [°]							
RPM	10	20	30	40	50	60	70	80
1200	2.411E-05	2.662E-05						
1400	2.300E-05	2.671E-05	2.751E-05	2.797E-05				
1600	2.166E-05	2.627E-05	2.714E-05	2.798E-05	2.855E-05	2.888E-05	2.922E-05	2.916E-05
1800	2.055E-05	2.578E-05	2.719E-05	2.805E-05	2.850E-05	2.880E-05	2.908E-05	2.886E-05
2000	1.955E-05	2.531E-05	2.756E-05	2.853E-05	2.889E-05	2.927E-05	2.948E-05	2.941E-05
2200	1.832E-05	2.461E-05	2.760E-05	2.846E-05	2.880E-05	2.920E-05	2.947E-05	2.933E-05
2400		2.398E-05	2.739E-05	2.829E-05	2.863E-05	2.904E-05	2.925E-05	2.916E-05
2600		2.295E-05	2.646E-05	2.766E-05	2.792E-05	2.838E-05	2.856E-05	2.858E-05
2800		2.231E-05	2.604E-05	2.744E-05	2.765E-05	2.816E-05	2.837E-05	2.833E-05
3000		2.161E-05	2.585E-05	2.756E-05	2.765E-05	2.836E-05	2.848E-05	2.853E-05
3200		2.106E-05	2.628E-05	2.842E-05	2.901E-05	2.948E-05	2.964E-05	2.974E-05
3400		2.025E-05	2.587E-05	2.855E-05	2.919E-05	2.971E-05	2.991E-05	2.992E-05
3600		1.959E-05	2.579E-05	2.873E-05	2.956E-05	3.015E-05	3.062E-05	3.054E-05
3800		1.886E-05	2.579E-05	2.905E-05	3.019E-05	3.096E-05	3.104E-05	3.138E-05
4000		1.821E-05	2.528E-05	2.888E-05	3.008E-05	3.090E-05	3.120E-05	3.138E-05
4200			2.451E-05	2.859E-05	2.983E-05	3.068E-05	3.105E-05	3.119E-05

For Fig.16, refer to Table C.11.

Table D.9: Cylinder Air Charge, refer to Fig.17

m_{ac} [kg]	θ [°]							
RPM	10	20	30	40	50	60	70	80
1200	3.520E-04	3.887E-04						
1400	3.357E-04	3.899E-04	4.016E-04	4.083E-04				
1600	3.163E-04	3.835E-04	3.962E-04	4.085E-04	4.169E-04	4.216E-04	4.267E-04	4.257E-04
1800	3.000E-04	3.764E-04	3.969E-04	4.095E-04	4.161E-04	4.205E-04	4.246E-04	4.214E-04
2000	2.854E-04	3.695E-04	4.024E-04	4.166E-04	4.218E-04	4.274E-04	4.304E-04	4.294E-04
2200	2.674E-04	3.593E-04	4.029E-04	4.155E-04	4.205E-04	4.263E-04	4.303E-04	4.282E-04
2400		3.501E-04	3.999E-04	4.130E-04	4.180E-04	4.240E-04	4.271E-04	4.257E-04
2600		3.350E-04	3.863E-04	4.039E-04	4.076E-04	4.144E-04	4.170E-04	4.173E-04
2800		3.257E-04	3.802E-04	4.006E-04	4.037E-04	4.111E-04	4.142E-04	4.137E-04
3000		3.155E-04	3.774E-04	4.024E-04	4.037E-04	4.140E-04	4.158E-04	4.165E-04
3200		3.075E-04	3.837E-04	4.150E-04	4.235E-04	4.304E-04	4.328E-04	4.342E-04
3400		2.957E-04	3.777E-04	4.169E-04	4.262E-04	4.337E-04	4.367E-04	4.368E-04
3600		2.860E-04	3.765E-04	4.195E-04	4.316E-04	4.402E-04	4.470E-04	4.459E-04
3800		2.753E-04	3.765E-04	4.242E-04	4.407E-04	4.520E-04	4.531E-04	4.582E-04
4000		2.659E-04	3.690E-04	4.217E-04	4.391E-04	4.512E-04	4.556E-04	4.581E-04
4200			3.578E-04	4.174E-04	4.355E-04	4.479E-04	4.534E-04	4.554E-04

Table D.10: Calculated MBT = $f(RPM,\theta)$, refer to Fig. 18

MBT	θ [°]							
RPM	10	20	30	40	50	60	70	80
1200	25.037	23.497						
1400	27.632	24.805	24.301	24.053				
1600	30.205	26.516	25.928	25.439	25.120	24.939	24.753	24.789
1800	32.164	28.262	27.403	26.946	26.711	26.552	26.416	26.521
2000	34.019	29.946	28.731	28.257	28.080	27.924	27.838	27.868
2200	33.458	29.507	28.126	27.769	27.631	27.489	27.392	27.442
2400		28.909	27.609	27.305	27.190	27.066	27.006	27.033
2600		27.793	27.089	26.758	26.688	26.561	26.513	26.506
2800		27.132	26.184	25.870	25.823	25.709	25.663	25.672
3000		26.039	25.193	24.899	24.884	24.765	24.748	24.741
3200		26.129	24.900	24.571	24.494	24.433	24.412	24.399
3400		26.124	24.765	24.371	24.294	24.238	24.216	24.215
3600		27.428	25.731	25.160	25.019	24.933	24.865	24.876
3800		30.167	27.840	26.870	26.568	26.383	26.365	26.282
4000		32.958	30.142	28.708	28.245	27.971	27.870	27.812
4200			32.626	30.654	30.003	29.639	29.480	29.422

Table D.11: Stoichiometric Fuel Conversion Efficiency = $f(RPM,\theta)$, refer to Fig. 19

η_f	θ [°]							
RPM	10	20	30	40	50	60	70	80
1200	0.343	0.350						
1400	0.357	0.355	0.351	0.354				
1600	0.361	0.361	0.366	0.356	0.352	0.361	0.354	0.360
1800	0.361	0.361	0.364	0.359	0.356	0.360	0.355	0.362
2000	0.355	0.359	0.362	0.361	0.364	0.357	0.354	0.361
2200	0.349	0.355	0.362	0.357	0.352	0.365	0.357	0.359
2400		0.353	0.358	0.359	0.357	0.363	0.359	0.358
2600		0.364	0.362	0.359	0.361	0.366	0.363	0.361
2800		0.363	0.366	0.362	0.364	0.369	0.366	0.366
3000		0.367	0.370	0.363	0.368	0.371	0.370	0.367
3200		0.374	0.368	0.365	0.363	0.371	0.369	0.369
3400		0.374	0.374	0.367	0.367	0.373	0.372	0.373
3600		0.375	0.372	0.370	0.370	0.376	0.371	0.372
3800		0.377	0.370	0.370	0.366	0.372	0.374	0.369
4000		0.368	0.367	0.367	0.362	0.367	0.369	0.370
4200			0.364	0.361	0.361	0.369	0.367	0.367

Table D.12: Cylinder Air Charge $= f(RPM, p_m)$, refer to Fig. 22

	p_m [kPa]											
RPM	*60*	*65*	*70*	*75*	*80*	*85*	*88*	*89*	*90*	*91*	*92*	*93*
1200						0.00036	0.00038	0.00039				
1400					0.00035	0.00038	0.00039	0.00040	0.00040	0.00040	0.00040	
1600				0.00032	0.00035	0.00038	0.00039	0.00039	0.00040	0.00040	0.00040	0.00042
1800			0.00030	0.00033	0.00036	0.00038	0.00039	0.00039	0.00040	0.00040	0.00041	0.00042
2000		0.00029	0.00032	0.00034	0.00037	0.00039	0.00040	0.00040	0.00041	0.00041	0.00042	0.00042
2200	0.00026	0.00029	0.00032	0.00034	0.00037	0.00039	0.00040	0.00041	0.00041	0.00041	0.00042	0.00042
2400					0.00037	0.00039	0.00040	0.00041	0.00041	0.00041	0.00042	0.00042
2600				0.00034	0.00036	0.00038	0.00039	0.00040	0.00040	0.00040	0.00041	0.00041
2800				0.00034	0.00036	0.00038	0.00039	0.00040	0.00040	0.00040	0.00041	0.00042
3000			0.00032	0.00034	0.00036	0.00038	0.00040	0.00040	0.00040	0.00040	0.00041	0.00042
3200		0.00031	0.00033	0.00035	0.00038	0.00040	0.00041	0.00042	0.00042	0.00043	0.00043	
3400	0.00028	0.00031	0.00033	0.00036	0.00038	0.00041	0.00042	0.00042	0.00043	0.00043	0.00044	
3600	0.00029	0.00032	0.00034	0.00036	0.00039	0.00042	0.00043	0.00043	0.00044	0.00044		
3800	0.00030	0.00032	0.00035	0.00037	0.00040	0.00043	0.00044	0.00045	0.00045	0.00045		
4000	0.00030	0.00032	0.00035	0.00038	0.00040	0.00043	0.00044	0.00045	0.00045	0.00046		
4200				0.00037	0.00040	0.00043	0.00044	0.00045	0.00045	0.00046		

REFERENCES

References

Ahlstrand, A., Haynes, J.H., "Ford Escort and Mercury Tracer Automotive Repair Manual," Haynes North America, Inc, Newbury Park, CA, 1996

Chang, R.T., "*A Modeling Study of the Influence of Spark Ignition Engine Design Parameters on Engine Thermal Efficiency and Performance*," M.I.T. Department of Mechanical Engineering, Sc.M. thesis, 1988

Dobner, D.J., "*A Mathematical Model for Development of Dynamic Engine Control*," pp.373-381, SAE Paper No. 800054, SAE Transactions, 1980

Fitzpatrick, T., "*Engine Start-up*", Hulett Road Engine Research Lab, 1995

Hempson, J.G.G., "The Automobile Engine 1920-1950", SAE paper No. 760605, vol. 85, 1976

Heywood, J.B., "*Internal Combustion Engine Fundamentals*", McGraw-Hill, New York, 1988

Huang, R.W., Velinsky, S.A., "*Spark Ignition Engine Modeling for Vehicle Dynamic Simulation*", DSC-Vol. 52, Advanced Automotive Technologies, pp. 369-378, ASME, 1993

Karnopp, D.C., Margolis, D.L, Rosenberg, R.C., "*System Dynamics: a Unified Approach,*" John Wiley & Sons, Inc., New York, 1990

Moskwa, J.J, Hedrick, J.K., "*Automotive Engine Modeling for Real-Time Control Applications,*" Proc. of the 1987 American Control Conference, 1987

Moskwa, J.J, Hedrick, J.K., "*Modeling and Validation of Automotive Engines for Control Algorithm Development,*" Paper presented at the Winter Annual Meeting of the American Society of Mechanical Engineers, San Francisco, 1989

Powell, B.K., Cook, J.A., "*Nonlinear Low Frequency Phenomenological Engine Modeling and Analysis*", Proceedings of the American Control Conference, pp. 332-340, 1983

Powell, J.D., "*A Review of IC Engine Models for Control System Design*", IFAC 10th Triennial World Congress, pp. 235-240, Munich, 1987

Reliance Electric Industrial Company, "*Dodge ® Engineering Catalog, Vol. 1.1,*" Greenville, SC, 1993

Ribbens, W.B., "*Understanding Automotive Electronics*", pp.150-152, Butterworth-Heinemann, Woburn, MA, 1998

Servati, H.B., Delosh, R.G., "*A Regression Model for Volumetric Efficiency,*" SAE Paper No. 860328, 1986

Tennant, J.A., Giacomazzi, R.A., Powell, J.D., Rao, H.S., "*Development and Validation of Engine Models via Automated Dynamometer Tests*", SAE Paper No. 790178, 1979